

A thermochronometric view into an ancient landscape: Tectonic setting, development, and inversion of the Paleozoic eastern Paganzo basin, Argentina

Eva Enkelmann^{1,*}, Kenneth D. Ridgway^{2,*}, Claudio Carignano^{3,*}, and Ulf Linnemann^{4,*}

¹DEPARTMENT OF GEOLOGY, UNIVERSITY OF CINCINNATI, 500 GEOLOGY PHYSICS BUILDING, CINCINNATI, OHIO 45221-0013, USA

²DEPARTMENT OF EARTH, ATMOSPHERIC, AND PLANETARY SCIENCES, PURDUE UNIVERSITY, 550 STADIUM MALL DRIVE, WEST LAFAYETTE, INDIANA 47907, USA

³CENTRO DE INVESTIGACIONES EN CIENCIAS DE LA TIERRA (CICTERRA), CONICET & UNIVERSIDAD NACIONAL DE CÓRDOBA, AVENIDA VÉLEZ SARSFIELD 1611, X5016GCA, CÓRDOBA, ARGENTINA

⁴SENCKENBERG NATURHISTORISCHE SAMMLUNGEN DRESDEN, MUSEUM FÜR MINERALOGIE UND GEOLOGIE, KÖNIGSBRÜCKER LANDSTRASSE 159, 01109 DRESDEN, GERMANY

ABSTRACT

In this study, we utilize multiple thermochronometric methods, including apatite and zircon fission track, (U-Th)/He, and zircon U-Pb, to evaluate the cooling history and provenance of sedimentary strata of the late Carboniferous to Late Permian eastern Paganzo basin and adjacent basement rocks (Argentina). The strata in the study area represent a long-lived, composite basin system that is interpreted to have experienced multiple periods of deformation, and to have received sediment from a number of different source terranes. These strata are well exposed in the Sierra de Chepes of west-central Argentina. New thermochronometric data and field observations, together with published data from the surrounding mountains, allow us to reconstruct: (1) the cooling history of the underlying basement rocks and the highlands surrounding the basin, (2) the thermal history of the source areas that provided sediment to the basin, and (3) the timing of structural inversion of the basin. Our data suggest that parts of the Sierra de Chepes were rapidly exhumed in Late Devonian–Carboniferous times; these exhuming areas supplied sediment to the adjacent basin. In contrast, the overlying red-bed strata originated from a slowly exhuming region located farther east or north of the basin within the Pampean orogenic belt or the Famatinian belt, respectively. Burial by latest Carboniferous and younger strata and an elevated geothermal gradient resulted in heating of the underlying Upper Carboniferous strata and underlying granitoid basement to temperatures between 80 °C and 140 °C. During Triassic time, the eastern Paganzo basin was structurally inverted; this event was marked by rapid cooling and may be related to regional extension and the development of rift basins to the west. The basement and the Upper Paleozoic strata of the eastern Paganzo basin in the study area have remained below 50 °C since latest Jurassic–Early Cretaceous times and are characterized by very slow cooling. Results of this study provide a thermochronometric view along an ~330 m.y. path defining the geologic evolution of the eastern Paganzo basin and the upper crust of west-central Argentina.

LITHOSPHERE, v. 6, no. 2, p. 93–107; GSA Data Repository Item 2014126

doi: 10.1130/L309.1

INTRODUCTION

Low-temperature thermochronometric methods like fission-track (FT) and (U-Th)/He dating of apatite and zircon have proven to be powerful tools to investigate rock exhumation in active mountain belts (e.g., Bernet et al., 2004; Blythe et al., 2007; Thiede et al., 2009; Enkelmann et al., 2010). In active tectonic settings, the spatial distribution of thermochronometric ages can be compared with observations of climate, topography, structures, and rock types, and this allows us to recognize correlations between crustal cooling and landscape evolution processes (e.g., Zeitler et al., 2001; Willett et al., 2003; Schuster et al., 2005). The reconstruction of tectonic

and surface processes in ancient mountain belts, however, is often much more challenging due to the long-term erosion of topography and related synorogenic strata, and the general modification of upper-crustal rocks over geologic time.

To continue to expand the application of thermochronometric tools to understand the evolution of ancient mountain belts, in this study we present new results from multiple thermochronometric methods (apatite and zircon FT and [U-Th]/He analysis) and zircon U-Pb ages from early Paleozoic bedrock and Upper Carboniferous to Permian detrital samples of the eastern Paganzo basin exposed in the Sierras de Chepes of west-central Argentina. The study area was chosen because it includes an exceptionally well-exposed Carboniferous paleo–glacier valley filled with Upper Carboniferous to Permian strata of the eastern Paganzo basin that were deposited on early Paleozoic basement (Sterren and Martinez, 1996; Socha

et al., 2006; Figs. 1 and 2). Our new thermochronometric and geochronometric results are discussed in context with published data from surrounding mountain belts of the Sierras de Pampeanas and allow the reconstruction of the Paleozoic through Cenozoic geological history of the eastern Paganzo basin and nearby basement exposures. Our study demonstrates that in some ancient settings, low-temperature thermochronometric approaches can yield meaningful first-order insights into the development of landscapes over long periods of geologic time.

GEOLOGICAL SETTING OF THE STUDY AREA

The Upper Carboniferous to Permian strata of the Paganzo basin crop out over a large part of west-central Argentina (Fig. 1; Fernandez-Seveso and Tankard, 1995). These strata are up to 1500 m thick and represent over 35 m.y. of

*E-mails: Enkelmann, corresponding author—eva.enkelmann@uc.edu; Ridgway—ridge@purdue.edu; Carignano—ccarignano@arnet.com.ar; Linnemann—ulf.linnemann@senckenberg.de.

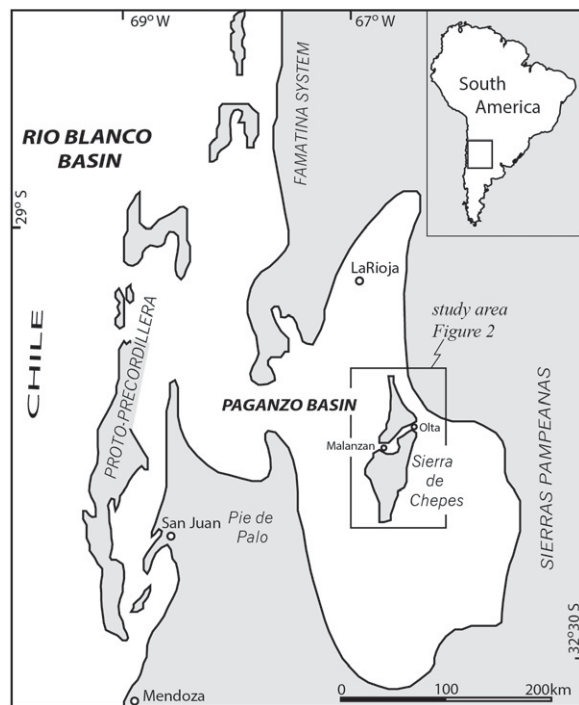


Figure 1. Late Carboniferous paleogeography of the Paganzo basin and Rio Blanco back-arc basin (modified after Limarino et al., 2006). Darker areas denote paleotopographic heights; white areas denote basins. Box shows the study area and map of Figure 2.

deposition in marine and continental environments (e.g., Fernandez-Seveso and Tankard, 1995; Limarino et al., 2006). The strata of the Paganzo basin contain a composite record of several different styles of deformation and tectonic settings, including Paleozoic strike-slip deformation, Mesozoic extension and inversion, and late Cenozoic contractional deformation (Fernandez-Seveso and Tankard, 1995; Ramos, 2010). Sedimentation in the eastern Paganzo basin started in the latest early Carboniferous to earliest late Carboniferous with the Serpukhovian–Bashkirian glaciation (Fig. 1; e.g., Limarino et al., 2006; Gulbranson et al., 2010). Glacial and deltaic strata related to this initial depositional stage are preserved in the paleo-glacier valley between the towns of Olta and Malanzan in the Sierra de Chepes (Fig. 1; Fig. DR1¹; Sterren and Martinez, 1996; Socha et al., 2006). We refer to these glacial and glacial-fluvial strata as part of the lower section of the Paganzo Group following the terminology of Azcuy and Morelli (1970). Overlying these Carboniferous strata, fluvial red-bed sandstone and conglomerate characterize the upper section of the Paganzo Group in the study area (Sterren and Martinez, 1996). The red-bed strata occur at the eastern and western flanks of the

Sierra de Chepes and in the topographic depression between the eastern and western parts of the paleovalley. These red beds were originally interpreted to be entirely Permian in age, but the start of deposition was recently revised to have been in the late Carboniferous, ca. 306 Ma (Gulbranson et al., 2010). We refer to these strata as the red beds of the upper section of the Paganzo Group in the text (Fig. 3).

The Sierra de Chepes consists of several smaller mountain ranges, including the Sierra de Los Llanos, the Sierra de Malanzan, the Sierra de Los Lujan, and the Sierra del Porongo,

which are all located in the west-central part of Argentina (Figs. 1 and 2). The Sierra de Chepes is today part of the basement uplifts of the Sierra de Pampeanas (Fig. 4), which are a product of Miocene to Holocene flat-slab subduction of the Nazca plate and Juan-Fernandez Ridge (e.g., Barazangi and Isacks, 1976, 1979; Ramos et al., 2002). The basement rocks of the Sierra de Pampeanas are a product of series of Paleozoic orogenies that developed through the accretion of different terranes into the proto-Andean margin of Gondwana. Three tectonic phases have been identified: the Early Cambrian Pampean (580–510 Ma), the Late Cambrian–Ordovician Famatinian (500–440 Ma), and the Devonian Achaian orogenic cycles (420–350 Ma) (e.g., Toselli and Aceñolaza, 1978; Aceñolaza and Toselli, 1981; Omarini, 1983; Ramos et al., 1986; Baldo et al., 1996; Rapela et al., 1998, 2007; Martino, 1999; Siegesmund et al., 2004, 2010; Steenken et al., 2004; López de Luchi et al., 2007; Drobe et al., 2009, 2011). The Sierra de Chepes is mainly composed of granitoid rocks dated at 497–477 Ma, and small (couple of meters thick) discontinuous exposures of metasedimentary rocks (Fig. 3; Pankhurst et al., 1998; Stuart-Smith et al., 1999).

METHODS

Samples

During a reconnaissance trip across the Sierras de Pampeanas, we collected six samples from strata of the eastern Paganzo basin and four samples from the underlying basement rocks in the Sierra de Chepes (Table 1; Figs. 2 and 3). Three of the bedrock samples are part of the paleovalley floor beneath the Carboniferous

TABLE 1. SAMPLE INFORMATION AND LOCATION

Sample	Longitude (°W)	Latitude (°S)	Rock description	Time of deposition/stratigraphic unit
Bedrock				
28TR2	66°26.610	30°46.161	Granite	
28TR4	66°22.526	30°39.126	Granite	
28TR6	66°31.516	30°30.617	Granite	
29TR3	66°17.051	30°39.116	Mafic gneiss	
Detrital				
29TR4	66°18.679	30°38.094	Sandstone with large dropstones	350–320 Ma; Malanzan Formation ¹ 324–318 Ma; Guandacol Formation (SI-1) ²
29TR6	66°20.591	30°38.544	Sandstone layer underneath big boulders	ca. 320 Ma; uppermost Malanzan Formation ¹ ca. 318 Ma; boundary SI-1/SI-2 ²
29TR7	66°21.730	30°38.826	Sandstone layers within fine sandstone and silt	315–305 Ma; Loma Larga Formation ¹ 318–311 Ma; Tupe Formation (SI-2) ²
28TR7	66°32.657	30°48.328	Sandstone layers within silt and mudstone	350–320 Ma; Malanzan Formation ¹ 324–318 Ma; Guandacol Formation (SI-1) ²
29TR2	66°16.785	30°38.395	Red-bed sandstone	<299; Permian
28TR1	66°30.776	30°47.283	Red-bed sandstone	ca. 270–306 Ma; late Carboniferous–Permian

Note: Stratigraphic units are shown in Figure 1. References: 1—Net and Limarino (1999); 2—Gulbranson et al. (2010).

¹GSA Data Repository Item 2014126, Figures DR1–DR5 and Tables DR1–DR6, is available at www.geosociety.org/pubs/ft2014.htm, or on request from editing@geosociety.org, Documents Secretary, GSA, P.O. Box 9140, Boulder, CO 80301-9140, USA.

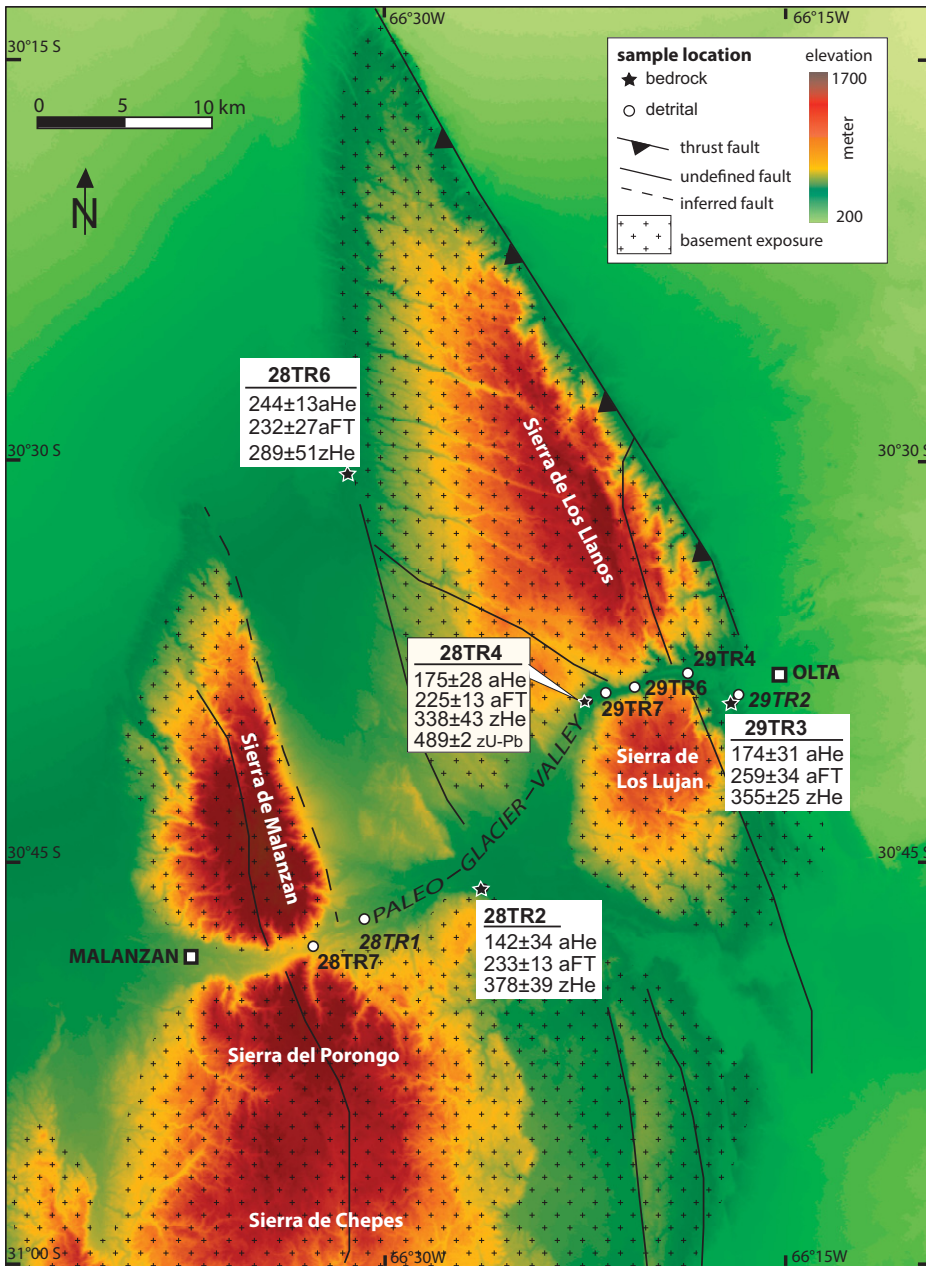


Figure 2. Digital elevation model of the Sierra de Chepes overlain by areas of basement exposure (cross pattern), all other areas are covered by Upper Carboniferous and younger sedimentary strata. The location of the samples and thermochronometric results of the bedrock samples are shown.

erous strata (28TR2, 28TR4, and 29TR3), and one sample represents the basement outside the paleovalley system, located ~25 km north (28TR6; Fig. 2). Four sedimentary samples are from the lower section of the Paganzo Group that is composed of Upper Carboniferous glacial (28TR7, 29TR4, and 29TR6) and glacial-fluvial (29TR7) strata within the paleovalley (Figs. 2 and 3). Two samples are from the upper section of the Paganzo Group and are composed of red-bed sandstones (28TR1 and 29TR2). The contact between the strata of the lower section

of the Paganzo Group and bedrock, as well as the U-shaped valley form that widens toward the west, is observed in the study region. In the Data Repository, we provide field pictures of the Upper and Lower Paganzo Group strata and observations of the contact between bedrock and strata (Fig. DR1 [see footnote 1]).

The four glacial and glacial-fluvial samples were collected at different sites within the paleo-glacier valley system from the base of the lower Upper Carboniferous strata (samples 29TR4 and 28TR7; Fig. 3). These samples are

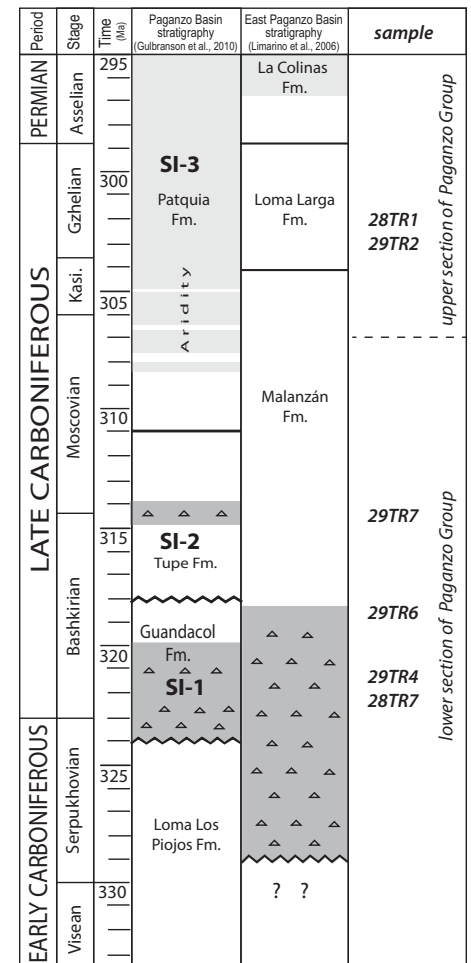


Figure 3. Stratigraphic section of the Paganzo Basin modified from Gulbranson et al. (2010). Dark-gray shading with triangle symbols indicates time of glacial deposits. Light-gray shading indicates sediments deposited in arid environment. Zigzag line indicates erosional contacts. SI-1, SI-2, and SI-3 are subunits defined by Gulbranson et al. (2010). On the right side, the sample IDs of this study are subdivided into the upper and lower sections of the Paganzo Group (Azcué and Morelli, 1970).

from the Malanzán Formation (350–320 Ma), which was defined for the Sierra de Los Llanos by Braccini (1946) and later included in the lower section of the Paganzo Group (Azcué, 1975; Andreis et al., 1986), and which is equivalent to the Guandacol Formation of Cuerda (1965) defined for the provinces of La Rioja and San Juan. These formations are equivalent to unit SI-1 of Gulbranson et al. (2010), who constrained the age at 324–318 Ma based on macroflora. Sample 29TR6 is from the top of the Malanzán Formation and was deposited at ca. 318 Ma near the contact with the Tupe Formation; the Malanzán Formation was defined for the La Rioja Province by Frenguelli (1944)

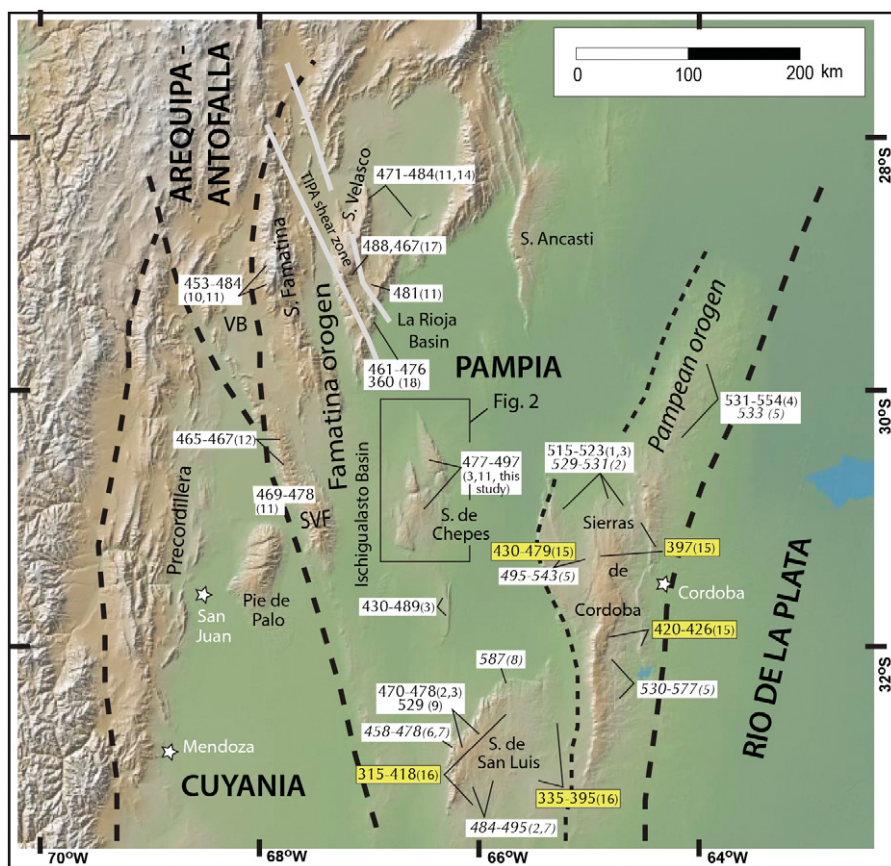


Figure 4. Topographic map showing the distribution of uplifted basement blocks of central-northwestern Argentina. VB—Vinchina Basin; SVF—Sierra de Valle Fertíl; TIPA—Tinogasta-Pituit-Antinaco. The crystallization ages for Paleozoic granitoids (regular numbers) and metamorphic rocks (italic numbers) are shown. The original sources of zircon and monazite dating are as follows: 1—Rapela et al. (1998); 2—Sims et al. (1998); 3—Stuart-Smith et al. (1999); 4—Schwartz et al. (2008); 5—Siegesmund et al. (2010); 6—Steenken et al. (2006); 7—González et al. (2004); 8—Drobe et al. (2009); 9—Söllner et al. (2000); 10—Dahlquist et al. (2008); 11—Pankhurst et al. (1998); 12—Rapela et al. (2001); 13—Dahlquist et al. (2007); 14—Báez et al. (2008); 15—Steenken et al. (2010); 16—Steenken et al. (2008); 17—Höckenreiner et al. (2003); 18—de los Hoyos (2011). Biotite K-Ar ages are shown in yellow boxes. Map is modified from Ramos et al. (2010).

and Cuerda (1965) and is equivalent to unit SI-2 of Gulbranson et al. (2010; Fig. 1 herein). Sample 29TR7 is from the Loma Larga Formation (315–305 Ma), defined for the Sierra de Los Llanos by Andreis et al. (1986), which is part of the Tupe Formation (SI-2 unit) that was deposited 318–311 Ma (Gulbranson et al., 2010; Figs. 2 and 3; Table 1). The two red-bed samples (28TR1 and 29TR2; Fig. 3) are from the Solca Formation, defined for the Sierra de Los Llanos by Andreis et al. (1986), and equivalent to the Patquia Formation defined for the provinces of La Rioja and San Juan by Cuerda (1965) (Fig. 3). Their depositional age is less well constrained but is interpreted to be between the late Carboniferous and the Early Permian (<306 Ma; Gulbranson et al., 2010). The red-bed strata in the eastern study area are assumed to be Permian in age (<299 Ma) based on fossilized trees

(Crisafulli and Herbst, 2008; Gulbranson, 2011, personal commun.).

All samples were crushed and sieved to grain sizes between 80 and 300 μm . After washing the samples, the apatite and zircon grains were separated using standard magnetic and heavy liquid separation.

(U-Th)/He Analysis

Clear apatite and zircon grains without inclusions and other impurities were selected from the bedrock samples using a binocular microscope. After documenting the grain dimensions, single grains were packed in Nb-tubes for (U-Th)/He analysis. In general, we analyzed 3–6 aliquots per sample. The samples were analyzed in the Patterson helium-extraction line at the University of Tübingen, which is equipped with a diode laser

to extract the gas. Apatite grains were heated for 5 min at 11 A, and zircon grains were heated for 10 min at 20 A. Each grain was heated and analyzed a second time to make sure that the grain was degassed entirely in the first step. The re-extracts generally showed <1% of the first signal. After helium analysis, the grain packages were sent to the University of Arizona at Tucson for U, Th, and Sm measurements using an inductively coupled plasma–mass spectrometer (ICP-MS).

The analytical errors of mass spectrometer measurements are generally very low (<2%); however, the alpha correction factor and the reproducibility of the sample age represent a much larger uncertainty on the (U-Th)/He age, and thus are a more honest display of the age precision. The scatter between the single-grain ages of the same sample is influenced by many factors, such as zoning of U and Th concentration, the alpha ejection, grain size, radiation damage, micro-inclusions, or any impurities. We report the single-grain ages with their analytical error and the mean (U-Th)/He age and the standard deviation as the sample error (Table 2). Due to the old (U-Th)/He ages, the range between single-grain ages appears large (tens of millions of years), but the sample age reproducibility (7%–18% for zircon and 5%–24% for apatite) is common for the (U-Th)/He method (e.g., Flowers et al., 2008; House et al., 2005; Stock et al., 2006; Hacker et al., 2011; Spotila and Berger, 2010). However, since the method is mostly applied to rocks that experienced Cretaceous–Cenozoic cooling, the absolute errors are usually small (<5 m.y.) and give the impression of a higher precision.

Apatite and Zircon Fission-Track Analysis

Fission-track analysis on apatite and zircon was carried out in the fission-track laboratory at the University of Tübingen. Apatite grains from both the bedrock and sedimentary samples were embedded in epoxy, grinded, and polished to expose internal surfaces of the apatites. The apatite mounts were etched in 5.5 M HNO_3 for 20 s at 21 °C to reveal the spontaneous tracks in apatite (Carlson et al., 1999). Afterward, the mounts were covered with a uranium-free muscovite external detector and irradiated with thermal neutrons at the research reactor facility at Garching (FRM-II, Germany). After irradiation, the external detectors were etched in 40% HF for 30 min to reveal the induced fission tracks. After etching, the external detector was placed back to its original position for track counting in apatite. Spontaneous and induced fission tracks were counted at a nominal magnification of $\times 1000$ using a Zeiss Axioskope microscope, by focusing first at the apatite surface and then up

TABLE 2. APATITE AND ZIRCON (U-Th)/He ANALYSIS

Sample	⁴ He (mol)	²³⁸ U (mol)	²³⁵ U (mol)	²³² Th (mol)	¹⁴⁷ Sm (mol)	Length (μm)	Width (μm)	eU	Uncorrected age (Ma)	Ft Alpha correction factor	Corrected age (Ma ± 1σ)	Mean age ± standard deviation (Ma)
Apatite												
28TR2	1.41E-13	5.90E-13	4.37E-15	1.22E-12	2.51E-12	283	133	16.5	123	0.808	152 ± 3.7	
28TR2	7.20E-14	4.84E-13	3.58E-15	6.24E-13	1.11E-12	335	111	14.5	88	0.788	111 ± 2.8	
28TR2	9.92E-14	3.09E-13	2.28E-15	8.32E-13	1.80E-12	255	109	15.7	150	0.768	195 ± 4.7	
28TR2	7.93E-14	4.60E-13	3.40E-15	7.58E-13	1.48E-12	332	149	8.2	95	0.831	115 ± 2.7	142 ± 34
28TR2	4.61E-14	2.53E-13	1.87E-15	3.60E-13	6.91E-13	230	108	11.9	104	0.766	136 ± 3.3	24%
28TR4	4.45E-13	2.14E-12	1.58E-14	5.56E-13	3.57E-12	258	152	36.3	149	0.830	179 ± 4.8	
28TR4	1.65E-13	1.11E-12	8.22E-15	1.17E-13	1.34E-12	186	128	35.6	110	0.791	139 ± 3.9	
28TR4	2.19E-13	9.50E-13	7.03E-15	2.02E-13	1.46E-12	212	118	32.2	166	0.784	211 ± 5.6	
28TR4	3.29E-13	1.54E-12	1.14E-14	2.99E-13	2.06E-12	299	148	23.5	155	0.832	186 ± 4.8	
28TR4	2.07E-13	9.53E-13	7.05E-15	2.11E-13	1.44E-12	271	131	20.5	157	0.811	193 ± 5.0	175 ± 28
28TR4	1.21E-13	6.95E-13	5.14E-15	2.84E-13	1.07E-12	239	157	12.3	121	0.831	145 ± 3.7	16%
28TR6	1.05E-13	3.63E-13	2.69E-15	1.50E-13	1.51E-12	221	106	15.3	197	0.766	256 ± 6.7	
28TR6	8.75E-14	3.52E-13	2.60E-15	1.60E-13	9.20E-13	175	94	24.0	170	0.729	232 ± 6.1	
28TR6	1.98E-13	6.96E-13	5.15E-15	2.62E-13	2.35E-12	271	131	15.5	196	0.810	241 ± 6.3	
28TR6	1.11E-13	3.41E-13	2.52E-15	1.84E-13	1.37E-12	239	157	6.2	215	0.830	259 ± 6.5	244 ± 13
28TR6	1.28E-13	4.60E-13	3.40E-15	1.53E-13	1.66E-12	299	154	6.7	193	0.837	230 ± 5.9	5%
29TR3	8.31E-14	3.05E-13	2.25E-15	8.81E-13	1.80E-12	192	126	15.8	124	0.780	159 ± 4.3	
29TR3	7.65E-14	2.70E-13	2.00E-15	5.83E-13	1.69E-12	228	123	11.1	142	0.787	181 ± 4.4	
29TR3	2.66E-14	1.27E-13	9.43E-16	2.89E-13	9.61E-13	266	92	8.2	103	0.736	140 ± 3.3	
29TR3	7.83E-14	1.44E-13	1.07E-15	8.97E-13	7.87E-13	233	114	11.0	171	0.767	222 ± 5.1	174 ± 31
29TR3	5.27E-14	1.99E-13	1.47E-15	4.22E-13	1.03E-12	257	132	6.3	134	0.803	167 ± 4.0	18%
Zircon												
28TR2	2.29E-12	5.05E-12	3.73E-14	2.39E-12		229	84	330	308	0.758	403 ± 10.2	
28TR2	5.13E-12	1.07E-11	7.94E-14	7.34E-12		252	93	543	312	0.780	397 ± 9.9	378 ± 39
28TR2	5.69E-12	1.39E-11	1.03E-13	6.76E-12		248	128	363	278	0.831	333 ± 8.8	10%
28TR4	2.63E-12	6.56E-12	4.85E-14	3.33E-12		216	75	575	272	0.731	369 ± 9.4	338 ± 43
28TR4	1.77E-12	4.60E-12	3.41E-14	2.72E-12		257	127	120	257	0.831	308 ± 8.1	13%
28TR6	3.62E-12	1.20E-11	8.89E-14	5.35E-12		265	81	727	208	0.756	273 ± 7.1	
28TR6	2.10E-12	5.72E-12	4.23E-14	3.09E-12		186	71	653	248	0.711	346 ± 8.9	289 ± 51
28TR6	2.82E-12	1.04E-11	7.70E-14	3.13E-12		219	92	572	193	0.775	248 ± 6.7	18%
29TR3	4.83E-12	1.30E-11	9.65E-14	4.90E-12		240	94	637	258	0.782	328 ± 8.5	
29TR3	1.79E-12	4.14E-12	3.06E-14	1.60E-12		181	104	220	299	0.788	377 ± 9.8	355 ± 25
29TR3	1.30E-12	3.04E-12	2.25E-14	2.11E-12		165	98	212	279	0.771	360 ± 9.8	7%

into the surface of the external detector (Jonckheere et al., 2003). The FT lengths and their angle to the crystallographic *c*-axis were measured on horizontal confined tracks using the same microscope equipped with a drawing tube and digitizing tablet and the FTstage 4.0 system provided by Trevor Dimitru.

Zircon grains were embedded in Teflon, polished, and etched in a eutectic solution of NaOH and KOH at 227–230 °C to reveal the spontaneous tracks. We prepared several mounts per sample and etched for various times ranging from 6 to 12 h. Between the etching steps, we checked the appearance of the etched tracks under the microscope to make sure that all zircon populations were properly etched. After etching, the zircon mounts were prepared for irradiation in the same way as the apatite mounts. Zircon fis-

sion tracks were counted under a nominal magnification of ×1000 (dry objective) using a Zeiss AxioImager M2M microscope equipped with an Autoscan stage system.

Zircon U-Pb Dating

We measured the zircon U-Pb age of individual zircon grains using laser-ablation (LA) ICP-MS at the Museum für Mineralogie und Geologie (GeoPlasma Laboratory, Senckenberg Naturhistorische Sammlungen Dresden). We analyzed 120 grains per sample for the two detrital samples (29TR2 and 29TR4) and 30 grains for the bedrock sample (28TR4).

Analytical techniques and settings of the analysis of U-Pb isotopes of magmatic and inherited zircon by LA-ICP-MS are described

as follows, and instruments settings are given in Table DR1 (see footnote 1). Zircons were analyzed for U, Th, and Pb isotopes by LA-ICP-MS techniques using a Thermo-Scientific Element 2 XR sector field ICP-MS coupled to a New Wave UP-193 Excimer laser system. A teardrop-shaped, low-volume laser cell constructed by Ben Jähne (Dresden) and Axel Gerdes (Frankfurt) was used to enable sequential sampling of heterogeneous grains (e.g., growth zones) during time-resolved data acquisition. Each analysis consisted of ~15 s background acquisition followed by 30 s data acquisition, using laser spot sizes of 25 and 35 μm, respectively. A common-Pb correction, based on the interference- and background-corrected ²⁰⁴Pb signal and a model Pb composition from Stacey and Kramers (1975), was carried out if necessary.

The necessity of the correction was judged based on whether the corrected $^{207}\text{Pb}/^{206}\text{Pb}$ value was located outside of the internal errors of the measured ratios. Discordant analyses were generally interpreted with care. Raw data were corrected for background signal, common Pb, laser-induced elemental fractionation, instrumental mass discrimination, and time-dependent elemental fractionation of Pb/Th and Pb/U using an Excel® spreadsheet program developed by Axel Gerdes (Institute of Geosciences, Johann Wolfgang Goethe-University Frankfurt, Frankfurt am Main, Germany). Reported uncertainties were propagated by quadratic addition of the external reproducibility obtained from the standard zircon GJ-1 (~0.6% and 0.5%–1% for the $^{207}\text{Pb}/^{206}\text{Pb}$ and $^{206}\text{Pb}/^{238}\text{U}$, respectively) during individual analytical sessions and the within-run precision of each analysis. Concordia diagrams (2 σ error ellipses) and concordia ages (95% confidence level) were produced using Isoplot/Ex 2.49 (Ludwig, 2001). The $^{207}\text{Pb}/^{206}\text{Pb}$ age was taken for interpretation of all zircons older than 1.0 Ga, and the $^{206}\text{Pb}/^{238}\text{U}$ ages were used for younger grains. For further details on analytical protocol and data processing, see Frei and Gerdes (2009). The Th/U ratios (Tables DR2 to DR4 [see footnote 1]) were obtained from the LA-ICP-MS measurements of investigated zircon grains. U and Pb content and Th/U ratio were calculated relative to the GJ-1 zircon standard and are accurate to ~10%.

RESULTS

This study presents data from four different thermochronometric systems that have been applied to two different kinds of samples, i.e., granitoid “bedrock” and sedimentary “detrital” samples. Each thermochronometric system yields ages of the sample that refer to the cooling below a certain closure temperature range and the thermal history within the temperature window where fission tracks anneal and helium diffusion occurs. In the simple case of continuous rock cooling through the temperature window where helium diffusion and FT annealing occur, the thermochronometric age represents the time of cooling below the closure temperature (Dodson, 1973). The zircon FT and (U-Th)/He system have the highest closure temperatures of 290–210 °C and 200–160 °C, respectively, depending on the cooling rate, grain size, and accumulated radiation damage (e.g., Yamada et al., 1995; Brandon et al., 1998; Reiners et al., 2002, 2004; Garver et al., 2005). The apatite FT and (U-Th)/He systems have lower closure temperatures of 110–100 °C and 80–50 °C, respectively (e.g., Green et al., 1986; Carlson et al., 1999; Schuster et al., 2006).

Because of the thermal sensitivity, subsequent heating due to burial or an increase in geothermal gradient can erase the cooling age of a sample. This property is particularly useful for sedimentary samples, because the thermochronometric results can be used to evaluate the postdepositional heating of sediment/strata in a basin setting. A reset sedimentary sample means that postdepositional burial was sufficient to heat the sample well above the closure temperature, which causes complete resetting of the original cooling signal due to the diffusive loss of helium or annealing of fission tracks. If heating was not high enough, but within the temperatures of partial helium retention or partial FT annealing, the sample is called partially reset and is characterized by apparent ages that are older and younger than the depositional age. An unreset sample is a sedimentary sample that has not been exposed to high temperatures, and the apparent ages, therefore, predate depositional age and provide information about the cooling of the source rock from which the sediment was eroded.

Bedrock Samples

Figure 2 displays the results of the bedrock dating using apatite and zircon (U-Th)/He and apatite FT analysis. Analytical results are given in Tables 2 and 3. The zircon (U-Th)/He ages are oldest, and the mean ages range from 378 ± 39 Ma to 338 ± 43 Ma within the paleo-glacier valley; the sample outside the valley yielded a younger zircon age of 289 ± 51 Ma (28TR6; Table 2). The apatite FT ages range from 259 ± 34 Ma to 225 ± 13 Ma, and the (U-Th)/He ages range from 142 ± 34 Ma to 175 ± 34 Ma for the three samples within the paleo-glacier

valley. The bedrock sample located to the north and outside the paleo-glacier valley yielded an apatite (U-Th)/He age of 244 ± 13 Ma, which is similar (within error) to the apatite FT age (232 ± 27 Ma) and suggests rapid cooling in the Triassic (Table 2).

The apatite FT and (U-Th)/He ages of the paleo-glacier valley basement postdate the late Carboniferous and thus indicate that they were heated to temperatures of at least within the apatite FT partial annealing zone after their Carboniferous surface exposure (Figs. 5A and 5B). This heating caused partial or full resetting of the apatite systems, which may be one reason that two samples failed the χ^2 test (FT ages) and show a larger scatter between single-grain aliquot measurements (apatite [U-Th]/He ages; Tables 2 and 3). Variations in grain size and radiation damage have been suggested as possible reasons for an observed spread between sample aliquots (e.g., Farley, 2002; Shuster et al., 2006). To investigate a possible correlation, we plotted the apatite and zircon (U-Th)/He ages of individual grains versus the effective uranium content (eU) and the diameter of the grain, but we did not find a correlation (Figs. DR2 and DR3 [see footnote 1]). We measured the diameter of the FT etch pits parallel to the crystallographic *c*-axis (Dpar) as a kinematic parameter for the apatite chemistry. Apatite chemistry may be responsible for different annealing behavior between grains (Carlson et al., 1999; Donelick and O’Sullivan, 2005). We did not observe variations among the Dpar values of individual grains in the bedrock samples, suggesting that the annealing behavior of the grains is similar.

Confined track length measurements were possible for two apatite samples (28TR2 and

TABLE 3. APATITE FISSION-TRACK ANALYSIS

Sample	No. grains	N_s	N_i	ρ_s (10^6 cm^{-2})	ρ_i (10^6 cm^{-2})	ρ_d (10^6 cm^{-2})	χ^2 (%)	Age (Ma $\pm 1\sigma$)	<i>n</i> length	Mean length (μm)	Dpar (μm)
Bedrock											
28TR2	49	2342	641	1.43	0.383	0.526	38	233 \pm 13	130	12.5 \pm 1.3	2.3 \pm 0.2
28TR4	41	2271	629	2.86	0.757	0.525	0	225 \pm 13	119	12.6 \pm 1.5	2.3 \pm 0.2
28TR6	13	373	100	1.21	0.341	0.524	51	232 \pm 27	–	–	–
29TR3	12	327	78	0.877	0.175	0.523	0	259 \pm 34	–	–	–
Lower section of Paganzo Group											
28TR7	112	8728	2387	2.03	0.551	0.522	0	245 \pm 8	334	12.7 \pm 1.4	2.6 \pm 0.2
29TR4	115	8438	2718	2.12	0.637	0.519	0	224 \pm 8	296	11.8 \pm 1.6	2.5 \pm 0.2
29TR6	105	6119	2026	1.76	0.590	0.516	0	209 \pm 7	173	12.7 \pm 1.4	2.6 \pm 0.2
29TR7	107	7716	2481	2.14	0.707	0.514	0	211 \pm 8	357	13.1 \pm 1.3	2.6 \pm 0.3
Upper Section of Paganzo Group											
29TR2	20	1396	443	2.49	0.832	0.520	0	215 \pm 20	77	13.6 \pm 1.3	3.0 \pm 0.4

Note: *n*—number of measured confined tracks; ρ_s —spontaneous track density; ρ_i —induced track density; N_s —number of spontaneous fission tracks; N_i —number of induced fission tracks; ρ_d —track density for the dosimeter glass (IRMM540), zeta calibration factor of $241 \pm 8 \text{ cm}^2$. The pooled age (bold) is calculated and can be interpreted as the sample cooling age; all other samples are mean ages (normal) calculated for samples that show more than one age population (see Table 4 for component ages).

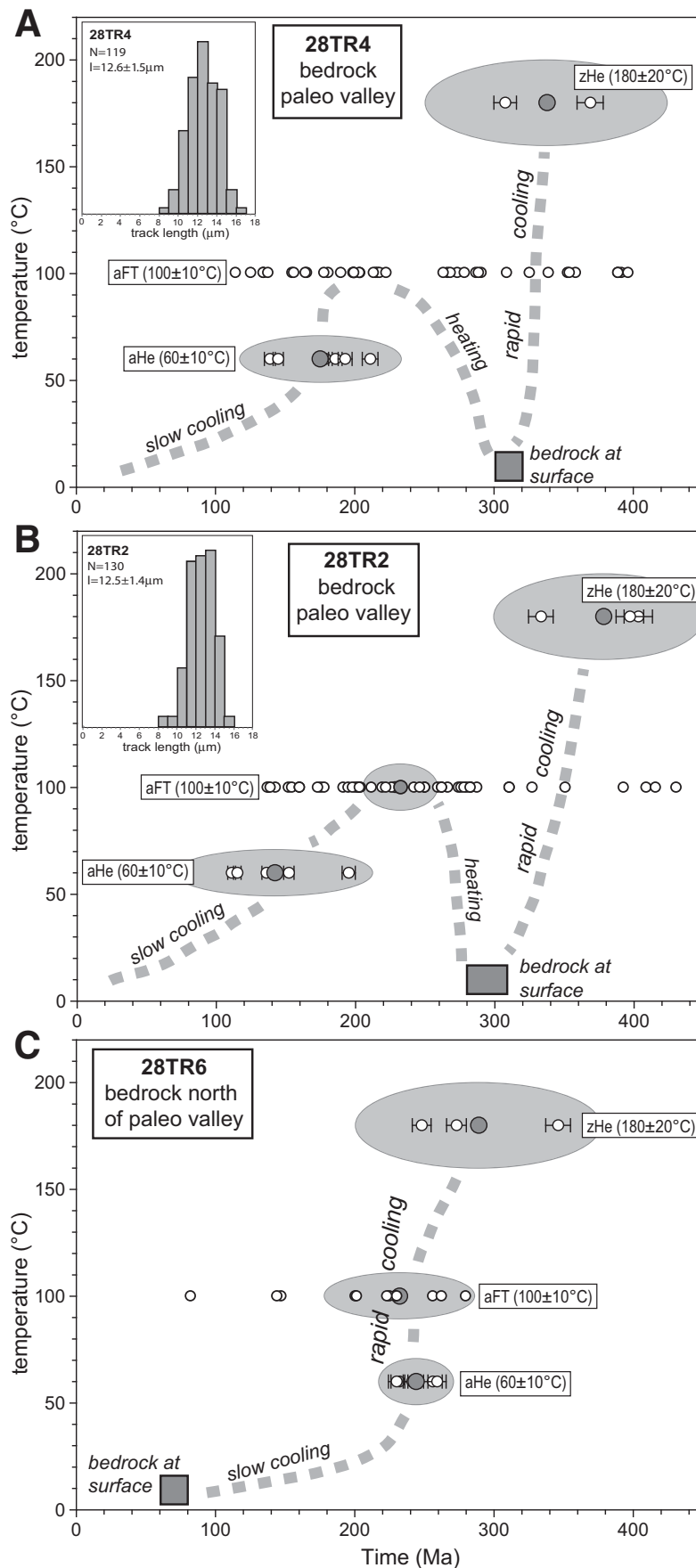


Figure 5. (A–C) Temperature-time diagram of bedrock samples. Displayed are the single-grain apatite and zircon (U-Th)/He ages (aHe and zHe) with 1σ error (white circles) and the mean age (gray circle). The large gray ellipses display the 2σ error of the mean (U-Th)/He ages (x-axis) and the range of the closure temperature (y-axis). The single-grain apatite fission-track (FT) ages (aFT) are shown in white circles, pooled age is shown in gray circle, and gray ellipses display 2σ error on the pooled age and the range in closure temperature for the samples that passed the χ^2 test (B and C). Gray box at ambient temperature indicates the time that bedrock was exposed, based on field observations that display sedimentary contact. The confined FT length distributions are displayed. N —number of measured confined tracks; l —measured mean track length and standard deviation.

28TR4) and yielded a unimodal length distribution with mean track lengths of $12.5 \pm 1.3 \mu\text{m}$ and $12.6 \pm 1.5 \mu\text{m}$ (Fig. 5). We present the apparent ages and spread in single-grain ages for the three thermochronometric systems in a temperature versus time diagram together with the field observations in Figure 5. Additionally, we analyzed the zircon U-Pb age of sample 28TR4, which yielded a concordia age of $489.3 \pm 1.7 \text{ Ma}$ (1σ ; Fig. DR5 [see footnote 1]). Sample 28TR6 is located north of the paleo-glacier valley, and the cooling ages differ from those samples collected in the valley. This sample was located at a much deeper crustal level during the early Carboniferous in comparison to those samples in the paleovalley. The mean ages and single-grain ages are presented, revealing the thermal history of the sample, in Figure 5.

Sedimentary Samples

For the detrital samples, we analyzed at least 100 grains per sample using the apatite and zircon FT method, and zircon U-Pb dating. The analytical details of single-grain measurements are given in the Data Repository (Tables DR2 to DR6 [see footnote 1]). The mineral separation process for the red-bed samples of the upper section of the Paganzo Group, however, did not yield any apatites for sample 28TR1 and only 20 apatite grains that could be analyzed for sample 29TR2. For the zircon FT analysis, we counted more than 100 grains for all samples, but one (29TR6), which yielded only 70 grains. Distributions of the grain ages from each sample were analyzed using a grain-age-deconvolution and binomial peak-fitting procedure (Galbraith and Green, 1990; Brandon, 1992, 1996; Galbraith and Laslett, 1993). The peak-fitting results are summarized in Table 4 and displayed in Figure 6.

TABLE 4. BINOMIAL PEAK-FITTING RESULTS OF THE DETRITAL APATITE AND ZIRCON FISSION-TRACK DATA

Sample	n	P1 (Ma)	P1 size (%)	P2 (Ma)	P2 size (%)	P3 (Ma)	P3 size (%)	
Zircon								
29TR4 z	106	340 ± 42	100					Not reset
29TR6 z	70	369 ± 46	100					Not reset
29TR7 z	104	363 ± 44	100					Not reset
28TR7 z	103	333 ± 40	100					Not reset
29TR2 z	105	432 ± 75	66	504 ± 70	34			Not reset
28TR1 z	105	185 ± 32	32	307 ± 41	68			Partially reset
Apatite								
29TR4 a	115	149 ± 8	44	253 ± 15	56			Reset
29TR6 a	105	155 ± 11	54	239 ± 21	46			Reset
29TR7 a	107	171 ± 10	72	265 ± 30	28			Reset
28TR7 a	112	142 ± 20	4	215 ± 90	69	322 ± 200	27	Partially reset
29TR2 a	20	133 ± 13	42	269 ± 25	58			Reset

Note: n—number of single grains analyzed; P—best-fit age populations in Ma with 1σ error, calculated using BINOMFIT 1.1 (Brandon, 1992). For zircons, a zeta calibration factor of 94 ± 11 a cm² was used together with IRMM541 uranium glasses.

Detailed tables of single-grain ages are provided in the Data Repository (see footnote 1).

With the exception of one sample (28TR1), the detrital zircon FT age distribution is generally older than the late Carboniferous deposition age, with peak ages ranging from 333 ± 40 Ma to 504 ± 70 Ma (Table 4). The detrital apatite FT ages are mostly younger than the deposition ages and are therefore reset (or partially reset), with mean apatite FT ages ranging from 209 ± 7 Ma to 245 ± 8 Ma (Table 3; Table DR5 [see footnote 1]). The apatite age distributions show generally two age populations, with the youngest age-population peak ranging between 171 ± 10 Ma and 133 ± 13 Ma and older populations with age peaks between 269 ± 25 Ma and 239 ± 21 Ma (Table 4). Sample 28TR7 yielded three age populations that peak at 142 ± 20 Ma, 215 ± 90 Ma, and 322 ± 200 Ma, thus indicating that some grains are not reset. This sample is therefore interpreted as partially reset (Table 4). The confined track length was measured on each sample, which yielded unimodal length distributions with a mean track length ranging from 11.8 ± 1.6 μm to 13.6 ± 1.3 μm (Table 3; Fig. DR4 [see footnote 1]). The track length distributions are well constrained, with ~300 confined tracks measured per sample. We could not find a difference between the track length distribution of grains that yield younger FT ages and the length distribution of grains with older FT ages.

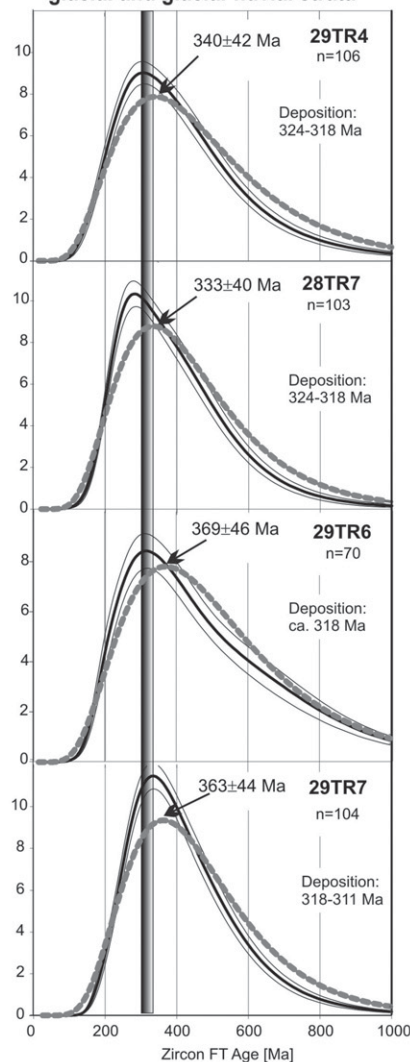
The zircon U-Pb age distributions of one glacial sample (29TR4) from the lower section of the Paganzo Group and one red-bed sample (29TR2) from the upper section of the Paganzo Group were measured and showed different age populations (Fig. 7). All single-grain ages and analytical results are given in the Data Repository (see footnote 1).

DISCUSSION

Cambrian to Carboniferous Cooling History

The granitoid basement rocks of the Sierra de Chepes are part of the Famatinian belt and underlie the eastern Paganzo basin. The basement rocks represent a continental magmatic arc and its metasedimentary host rocks that formed during the Ordovician along the proto-Andean margin of Gondwana (Aceñolaza and Toselli, 1981). Recent petrologic and geochronological studies of the basement rocks in the Sierra de Velasco, located north of our study area (Fig. 4), suggested a two-stage evolution for the exhumation of the Famatinian belt (de los Hoyos et al., 2011). Stage I suggests moderate exhumation rates (0.3–0.8 mm/yr) during the Early to Middle Ordovician driven by erosion of overthickened crust, followed by stage II, which is defined by long-lasting slow exhumation (0.01–0.09 mm/yr) from the Late Ordovician to early Carboniferous. This northern part of the Famatinian belt was additionally affected by postorogenic shallow magmatic intrusions in the early Carboniferous (monazite U-Pb: 360 Ma; de los Hoyos et al., 2011), but there is no evidence for

Lower Paganzo Group glacial and glacial-fluvial strata



Upper Paganzo Group red-bed strata

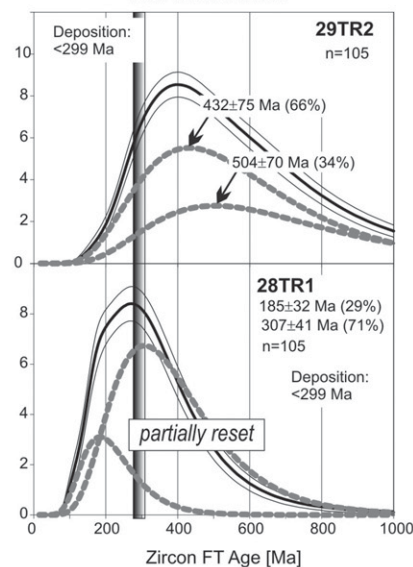


Figure 6. Probability density plot of the measured zircon fission-track (FT) age distribution (black line; thin lines show 1σ error) of the late Carboniferous to Permian sandy deposits. Age populations that fit to the measured age distributions have been found using a grain-age-deconvolution and binomial peak-fitting procedure (Galbraith and Green, 1990; Brandon, 1992, 1996). The modeled age population (thick dashed line) and the modeled peak age ±1σ error are given. n—number of measured grain ages.

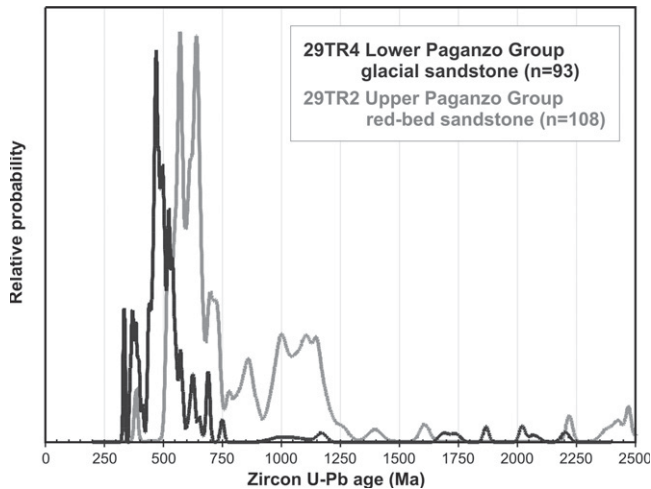


Figure 7. Probability density plot of the zircon U-Pb age distribution of a lower and upper section of the Paganzo Group sandstone sample.

magmatic activity during the Carboniferous in the Sierra de Chepes and farther south. The Sierra de Chepes basement predominantly consists of I-type and peraluminous granitoid rocks with Late Cambrian to Ordovician crystallization ages (Fig. 4; zircon U-Pb: 477–497 Ma; Pankhurst et al., 1998; Stuart-Smith et al., 1999; this study). Only small patches of greenschist- to amphibolite-grade metasedimentary rocks occur in the Sierra de Chepes with a suggested maximum depositional age of 510 Ma (Drobe et al., 2011), and an Early to Middle Cambrian age of metamorphism (e.g., Pankhurst et al., 1998; Dahlquist et al., 2005).

The bedrock and detrital samples of our study have been analyzed using four different low-temperature thermochronometric systems to reconstruct their thermal history in the upper crust. According to their low closure temperatures, we not only expect the apatite systems to yield the youngest ages, but also that the Paleozoic thermal record may have been easily erased and reset due to subsequent phases of heating and cooling. This is evident by the Mesozoic apatite cooling ages (Tables 2 and 3), which are discussed later herein (sections on “Late Paleozoic Heating and Triassic Cooling History” and “Jurassic through Cenozoic Cooling History and Basin Inversion”).

The zircon (U-Th)/He ages of the bedrock and detrital samples collected in the Carboniferous paleo-glacier valley provide information about Paleozoic cooling of the upper crust in this area. Additional constraints on the cooling history come from field observations that document a depositional contact between the late Carboniferous glacial strata and the granitoid basement rocks within the Olta-Malanzan paleo-glacier valley (Fig. 2; samples 28TR2, 28TR4, and 29TR3). This relationship implies that these three bedrock samples must have

been at surface temperatures before ca. 324–318 Ma, the age of the overlying glacial strata of the Guandacol Formation (SI-1; Gulbranson et al., 2010; Gulbranson, 2011; personal commun.). This is not the case for sample 28TR6, which is located north and outside of the paleo-glacier valley (Fig. 2)—it reveals cooling later in time as discussed later herein (section on “Late Paleozoic Heating and Triassic Cooling History”). The three bedrock samples reveal that the last cooling through $\sim 180^\circ\text{C}$ occurred in the Late Devonian through early Carboniferous (ca. 378–338 Ma; Table 2). We interpret this cooling to be related to rock exhumation, rather than lowering of the geothermal gradient, based on the fact that basement rocks were exposed at the surface by the end of the early Carboniferous. With surface exposure by ca. 324–318 Ma, our data suggest cooling from $\sim 180^\circ\text{C}$ to the surface in 60–14 m.y. Assuming a geothermal gradient of $25 \pm 5^\circ\text{C}/\text{km}$ and a surface temperature of $10 \pm 10^\circ\text{C}$, this suggests a moderate exhumation rate of 0.1–0.6 mm/yr during the early Carboniferous. Support for such moderate exhumation rates also comes from the detrital zircon FT and U-Pb ages of the Carboniferous strata discussed next. This result suggests that different parts of the Famatinian belt experienced different exhumation histories. While the Sierra de Velasco located to the north reveals exhumation with very slow rates during the early Carboniferous (de los Hoyos, 2011), the Sierra de Chepes were exhumed with rates an order of magnitude faster, possibly due to more surface uplift combined with efficient erosion by fluvial or glacial systems. Rapid rock exhumation is generally expected in regions of high uplift rates, creating local relief and elevation, which would also support the development of alpine glaciers that formed the preserved paleo-glacier valleys.

Late Carboniferous to Permian Cooling History and Provenance of Basin Strata

The combination of FT and U-Pb dating on detrital zircons of the late Paleozoic strata allows both identification of the provenance of the sediment supplied to the eastern Paganzo basin and also information about the cooling/exhumation history of the source terranes that provided sediment to this basin. The spread in the single-grain FT ages within the samples is generally wide (Fig. 6; Table DR6 [see footnote 1]), which is typical for detrital zircon FT dating due to the varying concentration of U and Th between individual zircon grains. The damage produced by the spontaneous fission of uranium and the alpha decay of uranium and thorium is accumulated at low temperatures and causes the transition from crystalline to amorphous (metamict) zircon. The resulting variation in the crystalline-to-metamict zircon properties causes a wide range of FT preservation between individual grains within a sample (Garver et al., 2005). That means the sample is a mixture containing low-retentive zircons and high-retentive zircons, which accumulate and anneal fission tracks at low or high temperatures, respectively (e.g., Seward and Rhodes, 1986; Carter, 1990; Garver et al., 2002, 2005). This temperature range can be from $<200^\circ\text{C}$ to $>350^\circ\text{C}$ (e.g., Tagami et al., 1998; Rahn et al., 2004; Garver et al., 2005). Despite the large spread in the zircon FT age distributions, we assume that the ages are not reset, consistent with the zircon (U-Th)/He age of the underlying basement, which are also not reset and reveal an early Carboniferous cooling.

The results of the zircon FT age distribution and binomial peak fitting reveal that all four samples of the lower section of the Paganzo Group yield only one age population that peaked in Late Devonian–early Carboniferous times, whereas the younger red-bed sample (29TR2) of the upper section yielded two populations with peaks in Silurian and Cambrian times (Table 4; Fig. 6). The other red-bed sample (28TR1) yielded zircon grains that are partially reset, with age population peaks that are both older and younger than the depositional age (Table 4; Fig. 6). That means the zircon ages of that sample do not provide cooling information from their source area, and this sample is therefore excluded for our discussion here.

The zircon FT age populations found in the sedimentary samples represent the average cooling signal in the catchment within the source region. There is a clear difference between the glacial and glacial-fluvial strata of the Lower Paganzo Group and the overlying red-bed sample of the Upper Paganzo Group. Each of the four samples from the Lower Paganzo Group

yields one age population with peak ages that range from 369 to 333 Ma. Taking these age populations and the deposition age, these samples suggest a lag time between 9 and 58 m.y. The lag time is the time the rock needed to cool below the zircon FT closure temperature, to be exhumed to the surface, and then to be eroded, transported, and finally deposited in the basin (e.g., Garver et al., 1999; Bernet and Garver, 2005). Similar to the basement samples, we can use the lag time to estimate the range of exhumation rates for the source area of these late Carboniferous strata. Using the zircon closure temperature of 250 ± 40 °C, an ambient temperature of 10 ± 10 °C, and a geothermal gradient of 25 ± 5 °C/km, the source area for the glacial strata was also exhumed with moderate to rapid rates ranging from 0.1 to 1.6 mm/yr. These exhumation rates overlap with those we estimated for the underlying basement (0.1–0.6 mm/yr) and suggest a proximal source area for the glacial strata. The range of exhumation rates derived from the detrital samples is larger due to the wide range of the zircon FT closure temperatures and the larger uncertainty associated with the zircon FT measurements. A local sediment source is supported by the observation of large granitic clasts and boulders in the diamictite at the base of the glacial strata; these are interpreted to have originated from corestones within local weathering profiles (Socha et al., 2006). Petrographic studies on the Carboniferous strata deposited near Malanzan also support a local source region from the Famatinian belt (Net and Limarino, 2006).

In contrast, much lower exhumation rates are derived for the red-bed sample (29TR2). The two age populations peak at 432 and 504 Ma, suggesting a lag time of at least 133 m.y. and 205 m.y. for each age peak (assuming a maximum deposition age of 299 Ma; Table 1). Using the same parameters for the closure temperature and the geothermal gradient as above, the sediment source area for this upper section of the Paganzo Group was an area with exhumation rates on an order of magnitude lower (0.03–0.1 mm/yr) than the strata of the lower section of the Paganzo Group and underlying basement rocks. Alternatively, the sediment source area may have experienced higher exhumation rates, but the amount of rock exhumation was not enough (>6–14 km) to exhume rocks from below the closure temperature depth. In any case, the zircon FT data suggest that the source area for the red-bed strata was different and located farther away than that for the underlying glacial and glacial-fluvial strata. This is also supported by the fact that the red beds are interpreted as having been deposited in braided river environments (Limarino et al., 2006) and

yielded two distinct zircon FT age populations, suggesting that the fluvial catchment was probably large and consisted of source areas with different exhumation histories.

To identify possible source regions, we can compare the zircon FT age populations with published biotite K-Ar cooling ages from the surrounding areas (Fig. 4). Biotite K-Ar ages refer to cooling below ~ 350 °C and are commonly used to study metamorphic processes (McDougall and Harrison, 1999, and references therein). Devonian and Carboniferous biotite cooling ages (418–315 Ma; Steenken et al., 2010) have been reported from gneiss, mylonite, and pegmatite of the Sierra de San Luis, which is located south of our study area and is part of the Famatinian belt (Fig. 4; Steenken et al., 2008). Carboniferous apatite U-Pb and biotite Rb/Sr ages have also been reported from meta-granodiorite and mylonite of the Tinogasta-Pituil-Antinaco shear zone (Höckenreiner et al., 2003). This NNW-trending shear zone separates the Pampean and the Famatinian belt and is exposed today north of the Sierra de Chepes. This suggests that sediment in the glacial and glacial-fluvial strata may have originated from the nearby Famatinian belt (Sierra de Chepes) or the Tinogasta-Pituil-Antinaco shear zone. In contrast, Ordovician and Silurian biotite cooling ages (480–400 Ma) have been reported from gneiss and mylonite of the Sierras de Cordoba located east of the study area, which are part of the Pampean orogenic belt (Fig. 4; Steenken et al., 2010). Slow rates of exhumation, comparable to those determined for the red-bed strata (29TR2) in our study area, have been suggested for the northern part of the Famatinian belt in the Sierra de Velasco during Late Ordovician to Carboniferous time (de los Hoyos et al., 2011).

The interpretation of two different source regions for the lower and upper sections of the Paganzo Group of the eastern Paganzo basin based on zircon cooling ages is also supported by the difference in the zircon crystallization ages between sample 29TR4 (glacial) and 29TR2 (red bed). The diagram in Figure 7 displays the probability density plot of the zircon U-Pb ages and shows that the glacial sample has a main population at 440–550 Ma, whereas the red-bed sample is composed of older zircons with main populations at 530–700 Ma and 980–1160 Ma (Fig. 7). The glacial sample (29TR4) reveals three grains out of 120 grains (2.5%) that yielded ages between 330 and 340 Ma, which indicate that early Carboniferous magmatic sources were not dominant. Comparing these zircon U-Pb age distributions with crystallization ages reported from Paleozoic granitoids and metamorphic belts in NW Argentina, we find that the Famatinian orogenic belt and

the protolith of the Tinogasta-Pituil-Antinaco shear zone mylonite have ages that are similar to the ages of zircons found in the glacial strata (29TR4; e.g., Pankhurst et al., 1998; Sims et al., 1998; Stuart-Smith et al., 1999; Höckenreiner et al., 2003; González et al., 2004; Steenken et al., 2006). A proximal source area is further supported by the U-Pb ages we determined for the bedrock sample 28TR4, which yielded an intrusion age of 489 Ma (Fig. 2; Data Repository [see footnote 1]), and other U-Pb ages reported from the Sierra de Chepes granitoids (477–497 Ma) and metasedimentary strata (500–650 Ma; Pankhurst et al., 1998; Drobe et al., 2011). In contrast, the zircon U-Pb ages of the red-bed sample suggest a source area located farther east of the Paganzo basin in the Sierras de Cordoba within the Pampean orogenic belt (Fig. 4; e.g., Rapela et al., 1998; Sims et al., 1998; Schwartz and Gromet, 2004; Schwartz et al., 2008; Siegesmund et al., 2010). In summary, a rapidly exhuming source located near the eastern Paganzo basin supplied sediment to the basin during Upper Carboniferous deposition, whereas a different source, located farther east of the basin, supplied sediment to the basin during the latest Carboniferous and Permian.

Late Paleozoic Heating and Triassic Cooling History

As expected, the apatite FT and (U-Th)/He cooling ages are younger than the zircon ages due to their lower closure temperatures. The apatite ages of the basement samples and the overlying strata, however, are also younger than the depositional age of the late Carboniferous to Permian strata (apatite FT: 259–225 Ma and apatite [U-Th]/He: 175–142 Ma; Fig. 2; Tables 1 and 2). This suggests that the basement and the overlying Paleozoic strata were heated after their surface exposure and deposition, respectively, to temperatures <160 °C, the lower temperature limit for the zircon (U-Th)/He closure temperature. This heating caused a partial and/or total loss of the previously accumulated daughter products in apatite (i.e., diffusion of helium and annealing of fission tracks), but not in zircon.

The unimodal length distributions of the five detrital samples (11.8 μm to 13.6 μm ; Table 3; Fig. DR3 [see footnote 1]) generally support the interpretation of full resetting of the apatite FT system; however, the large spread observed in the age distribution suggests that partial resetting of the apatite is also a likely interpretation. A partially reset sample is indicated by a bimodal and/or very broad length distribution with shorter tracks (e.g., Gleadow et al., 1986; Green et al., 1989). The binomial peak fitting

found generally two age populations with ages postdating deposition. Only one sample 28TR7 (westernmost sample, Fig. 2) yielded a third population that predates deposition and thus is clearly a partially reset sample. The unimodal length distribution of the underlying bedrock suggests maximum heating during Permian time to temperatures in the lower part of the apatite partial annealing zone, probably between 80 °C and 140 °C, followed by cooling (Figs. 5A and 5B).

Previous studies of the Upper Paleozoic strata in the Paganzo basin suggested sedimentation with a general thinning of the strata toward the east. Based on the interpretation of seismic profiles in the La Rioja Basin located to the north (Fig. 4), Fisher et al. (2002) suggested a maximum thickness of 800 m for the Upper Paleozoic strata. Fernandez-Seveso and Tankard (1995) estimated up to 2000 m thickness for the Upper Carboniferous Guandacol Formation and up to 730 m of Permian strata. In total, the estimated thickness of Upper Paleozoic strata appears insufficient to bury the basement to depths with temperatures more than 80 °C for a normal geothermal field. It is possible that estimates of the late Paleozoic strata thickness are too low due to subsequent erosion. We, however, suggest a combination of basement burial by Upper Paleozoic strata and an increase in the geothermal gradient as the probable reasons for the heating of the basement rocks. The southwestern margin of Gondwana was affected by widespread magmatic activity throughout the late Carboniferous to Permian due to major geodynamic reorganization from convergent plate margin to extensional regimes (e.g., Uliana and Biddle, 1988; Mpodozis and Kay, 1992; Kleiman and Japas, 2009; Ramos, 2010). This magmatic event is represented by the Choiyoi igneous province, which covers an area of ~500,000 km² of western Argentina and eastern Chile, with a thickness of up to 2000 m (e.g., López-Gamundí, 2006; Strazzere et al., 2006; Kleiman and Japas, 2009; Rocha-Campos et al., 2011). This large magmatic event must have, undoubtedly, influenced the geothermal structure of the Sierra de Chepes region.

Based on this reasoning, we suggest that the detrital apatite FT ages are reset (except sample 28TR7). The older of the two apatite FT age populations found in the reset samples ranges from 269 ± 25 Ma to 239 ± 21 Ma and is similar to the underlying bedrock apatite FT ages, which range from 259 ± 34 Ma to 225 ± 13 Ma. All these ages indicate that cooling occurred in the latest Permian through Triassic after the late Paleozoic burial/heating event (Tables 2 and 3). The Triassic cooling is supported by the bedrock sample north of the paleo-glacier valley

(28TR6; Fig. 2), which yielded similar apatite FT and (U-Th)/He ages of 232 ± 27 Ma and 244 ± 13 Ma, respectively, suggesting a phase of rapid cooling in the Triassic (Tables 2 and 3). The zircon (U-Th)/He age of the same sample is 289 ± 51 Ma (Table 2). The entire temperature-time path of this sample suggests rapid cooling in the Permian through Triassic from temperatures >180 °C to below ~45 °C (Fig. 5C).

The Triassic Ischigualasto Basin (Fig. 4) could be a possible sink for the eroded “missing” strata that may have buried the currently exposed Upper Carboniferous strata. This rift basin formed during regional extension at the beginning of Gondwana breakup and contains up to 6 km of clastic strata (Milana and Alcober, 1994; Stipanovic, 2002). The Ischigualasto Basin formed just west of the Sierra de Chepes and is characterized by a thick section of clastic strata and basalt flows (Gonzalez and Toselli, 1975; Valencio et al., 1975; Milana and Alcober, 1994; Stipanovic, 2002; Zerrass et al., 2004). The Sierra de Chepes itself is considered to have been a highland at this time, which is supported by our temperature-time paths of the basement samples outside and inside the paleo-glacier valley (Fig. 5). Evidence for late Carboniferous–Permian heating also comes from a granitoid sample of the Sierra de Cordoba, located east of our study (Fig. 4). The K-Ar analysis of muscovite and potassium feldspar suggests cooling well below 120 °C at 320 Ma, followed by a slight heating event that did not exceed 120 °C at 265 Ma (Jordan et al., 1989; Richardson et al., 2013).

Jurassic through Cenozoic Cooling History and Basin Inversion

The cooling paths incorporating all three thermochronometric systems per sample suggest that since Triassic time, the bedrock has been below 60–50 °C and has experienced very slow cooling (0.07–0.02 °C/m.y.) to ambient temperatures (Fig. 5). A long-lasting very slow cooling trend from the Triassic through Cretaceous time is also indicated by the wide spread in the bedrock apatite (U-Th)/He ages (244–142 Ma; Table 2) and the youngest age population found in the detrital apatite FT samples, which cluster between 171 and 133 Ma (Table 4).

A slightly different result is indicated by the sample collected outside the paleo-glacier valley (28TR6). The smaller spread in the apatite (U-Th)/He ages suggests that cooling to temperatures below the partial helium retention zone (~45 °C) occurred already in the Triassic, followed by steady-state conditions with no significant heating or cooling. Evidence for surface exposure of the basement near the location of

sample 28TR6 comes from field observations that show Upper Cretaceous strata overlapping the basement. These strata were deposited in Campanian times, based on dinosaur, crocodile, and turtle biostratigraphy (80–70 Ma; Fiorelli et al., 2011).

As stated already, the Sierra de Chepes is today part of the Sierras de Pampeanas, which consists of uplifted basement blocks with high topography up to 3000 m elevation (e.g., Sierra de Velasco) and 1500 m in the study area. Low-temperature thermochronometers have been used in the past to quantify the amount and timing of Cenozoic deformation within the Sierra de Pampeanas (e.g., Jordan et al., 1989; Coughlin et al., 1998; Richardson et al., 2013). Jordan et al. (1989) dated samples from the Sierras de Famatina, Velasco, and Ancasti, located north of our study area, and the Sierra de Cordoba, located to the east. Apatite FT ages range between 237 and 115 Ma and are interpreted to reflect a long steady state in the upper part of the partial annealing zone before late Cenozoic cooling (Jordan et al., 1989). Apatite FT dating of basement rocks collected from elevation profiles in the western ranges of the Sierra de Pampeanas and west of the Sierra de Chepes (e.g., Sierra de Velle Fertil, Sierra de Famatina, Sierra de Maz; Fig. 4) records a wide range of ages from 300 to 7 Ma (Coughlin et al., 1998). Based on these data, it was suggested that Andean deformation started during the late Paleocene–middle Eocene, which was followed by burial/heating due to sedimentation in the developing Andean foreland basin (Coughlin et al., 1998). The Juan-Fernandez Ridge flat-slab subduction caused Neogene basement-involved deformation of the Sierras de Pampeanas, creating topography of >1500 m elevation in the eastern, and >3000 m elevation in the western and northern ranges. Due to the lack of Neogene cooling ages in the eastern ranges, and only a few Neogene ages exposed in the western ranges, it is generally assumed that basement uplift did not result in rock exhumation exceeding 2–3 km (Jordan et al., 1989; Coughlin et al., 1998). Recent studies of illitization processes in the Neogene Vinchina Basin, located farther northwest of the Sierra de Chepes (Fig. 4), have suggested a very low geothermal gradient of 15–18 °C/km (Collo et al., 2011), which would allow a much larger amount of rock exhumation without exhumation of rocks from below the apatite (U-Th)/He or FT closure temperature. Davila and Carter (2013) revisited published apatite FT data from the western ranges of the Sierra de Pampeanas (located west and north of our study) and suggested substantial rock exhumation across the foreland region due to flat-slab subduction and lowering of the geothermal gra-

dient. In summary, the new thermochronometric results together with those published from the eastern ranges reveal a time of very slow cooling since the Mesozoic.

SUMMARY

By employing multiple thermochronometric systems to analyses of a suite of bedrock and sedimentary samples in west-central Argentina, we are able to reconstruct the thermal evolution of the basement rocks of the eastern Paganzo basin, identify two distinct sediment source areas that supplied sediment to the basin, and establish the timing of basin inversion. These data provide a thermochronometric view into an ancient landscape and record its evolution from Paleozoic time to the present. A summary of our observations and interpretations is given in Figure 8.

The zircon cooling ages provide estimates of Paleozoic exhumation rates for both the base-

ment rocks of the Sierra de Chepes and the sediment source areas of the Carboniferous glacial and glacial-fluvial strata in the eastern Paganzo basin. For the Sierra de Chepes and the nearby surrounding terranes that provided sediment to the late Carboniferous basin, we derived long-term ($>10^6$ yr) exhumation rates of 0.1–1.6 mm/yr for Late Devonian–Carboniferous times. These exhumation rates, derived from zircon thermochronometric systems, are comparable to those reported from tectonically active mountain ranges like the European Alps (0.2–0.3 mm/yr; Bernet et al., 2009), the Himalayas (0.3–1.4 mm/yr; e.g., Bernet et al., 2006; Blythe et al., 2007; Thiede et al., 2009; Enkelmann et al., 2011), and the Andes (0.2–1.3 mm/yr; e.g., Garver et al., 2005). In contrast, exhumation rates are an order of magnitude lower in ancient, currently not tectonically active mountain belts, such as the Appalachians (0.07–0.08 mm/yr; Roden-Tice and Tice, 2005), Scandinavia (<0.02 mm/yr; e.g., Hendriks et al., 2007, and

references therein), or Northern (0.02–0.05 mm/yr; Lisker et al., 2006) and Southern Victoria Land in Antarctica (0.08–0.1 mm/yr; Fitzgerald et al., 2006). All of these active and ancient orogens constitute mountain belts with >1500 m peak elevations, and all of them are glaciated or have been glaciated throughout the Quaternary. However, the average long-term exhumation rates differ by an order of magnitude between the tectonically active and ancient “inactive” mountain belts. Carving deep glacial valleys into a tectonically inactive mountain belt often produces impressive topographic relief and may also result in young cooling ages of the lower-temperature systems such as apatite (U-Th)/He, but it does not result in the rapid exhumation of rocks originating from greater depths below the closure temperatures of zircon FT or the (U-Th)/He system. However, this is the case when efficient fluvial or glacial erosion removes the actively uplifting surface in tectonically active mountain belts. In these types of settings, active mountainous regions show higher relief with peak elevations of >4000 m. We thus could reasonably speculate that this region of the Sierra de Chepes and parts of the orogenic Famatinian belt must have been significant mountain ranges that were tectonically active in the Carboniferous. Based on the results of our study, we suggest that at least parts of the orogenic belts in west-central Argentina were characterized by surface uplift and rapid rock exhumation with amounts that were sufficient to expose rocks from depths below the zircon FT closure temperature. In contrast, the area located farther east of the Paganzo basin (Pampean orogenic belt), which delivered sediment to the red-bed strata of the upper section of the Paganzo Group, was tectonically inactive in the late Carboniferous through Permian and probably was characterized by much lower topography relative to the Famatinian belt. Our findings show that we can reconstruct the first-order late Carboniferous topography of the eastern Paganzo basin and surrounding highlands; our study provides an example of the type of information that can be acquired with thermochronometric data from older landscapes.

The interpreted deposition of at least 2.5 km of strata on top of the currently exposed Upper Carboniferous paleovalley strata also indicates that during the Permian, the area of the Sierra de Chepes was subsiding and part of a sedimentary basin. Inversion of the eastern Paganzo basin, marked by rapid cooling and exhumation, occurred in Triassic–Early Jurassic time with the beginning of Mesozoic rift development associated with opening of the Atlantic Ocean (Uliana and Biddle, 1988; Uliana et al., 1989; Zerfass et al., 2004). Since that time, the

OBSERVATIONS	INTERPRETATION
L. Devonian to Carboniferous	
<ul style="list-style-type: none"> - bedrock zircon (U-Th)/He ages and detrital zircon FT ages - contact between basement and glacial strata, depositional age - comparison with biotite K-Ar and zircon U-Pb ages from other areas 	<ul style="list-style-type: none"> - rapid exhumation of Sierra de Chepes basement - alpine glaciation starts at ~324 Ma - local and rapidly exhuming source for glacial strata - source with exhumation rates of 0.1–1.6 mm/yr in the Famatinian belt
Permian	
<ul style="list-style-type: none"> - reset and partial reset of apatite ages in bedrock and strata - unreset zircon systems - comparison with biotite K-Ar and zircon U-Pb ages from other areas - depositional age of red-beds 	<ul style="list-style-type: none"> - heating of basement and strata to $>80^\circ$ and $<140^\circ\text{C}$ - increased geothermal gradient due to widespread magmatic activity - subsidence of Sierra de Chepes, deposition of red-bed strata - distant and slowly exhuming source for red-bed strata - source with exhumation rates of <0.1 mm/yr in the Pampean belt
Triassic	
<ul style="list-style-type: none"> - apatite FT ages of sediment and bedrock - lack of sedimentary strata in the Sierra de Chepes 	<ul style="list-style-type: none"> - basin inversion and uplift - exhumation of Sierra de Chepes - cooling of basement and strata to $<100^\circ\text{C}$ - formation of the Ischigualasto Basin, deposition of 6 km strata - beginning of regional extension
Late Jurassic to Oligocene	
<ul style="list-style-type: none"> - apatite (U-Th)/He ages - observed peneplains in the Sierra de Pampeanas 	<ul style="list-style-type: none"> - slow cooling of basement and cover strata - rocks are near the surface $<45^\circ\text{C}$ - formation of peneplain - no major cooling or heating
Miocene to Recent	
<ul style="list-style-type: none"> - topography with uplifted peneplain - active seismicity - no apatite cooling ages - exposed paleo-glacial valley and remaining strata - lack of significant young sediments 	<ul style="list-style-type: none"> - flat-slab subduction causes uplift of the Sierra de Chepes - exposure of paleo-glacier valley - uplifted peneplain at ~1500m elevation - no significant rock exhumation [<2 km]

Figure 8. Summary of observations and interpretations for the eastern Paganzo basin since Paleozoic time. FT—fission track.

strata of the Paganzo basin and related basement rocks have been at near-surface temperatures, and the region has experienced very slow cooling. These findings are consistent with documentation of Mesozoic peneplain surfaces that are preserved in the eastern Sierra Pampeanas (Jordan et al., 1989; Carignano et al., 1999). The Sierras Pampeanas are characterized today by active basement-involved deformation due to flat-slab subduction of the Juan Fernandez Ridge (Richardson et al., 2012). Neogene basement uplift has created topography of >1500 m elevation in the eastern Sierras Pampeanas, but it has not caused significant rock exhumation, which could be detected with low-temperature thermochronometric data (Jordan et al., 1989; Richardson et al., 2013). Thermochronometric studies in the Sierra de San Luis (located south of the study area) also suggest that the rocks were already near the surface in the Late Cretaceous and that the amount of sediments eroded since that time is <450 m (Löbens et al., 2011). In summary, our thermochronometric reconstruction of the geologic development of the Paleozoic Paganzo basin and related basement rocks demonstrates the applicability of multiple thermochronometric techniques to older settings that may have experienced multiple stages of both deformation and provenance over long periods of geologic time.

ACKNOWLEDGMENTS

We thank Roberto Donato Martino, Tonya Richardson, Hersh Gilbert, Mario Gimera Lopez, and Yamila Dubokovic for their help during field work. E. Enkelmann thanks E.L. Gulbranson for helpful discussion about the Paganzo stratigraphy. E. Enkelmann also thanks P. Reiners for U, Th, and Sm measurements. Ridgway's involvement in this project was supported by a National Science Foundation grant to Hersh Gilbert. The paper benefited from insightful and constructive comments from Martin Danisik and three anonymous reviewers.

REFERENCES CITED

- Aceñolaza, F.G., and Toselli, A.J., 1981, Geología del Noroeste Argentino: Publicaciones Especiales de la Facultad Ciencias Naturales, Universidad Nacional de Tucumán, v. 1287, p. 1–212.
- Andreis, R.R., Archangelsky, S., and Leguizamón, R.R., 1986, El paleovalle de Malanzán: Nuevos criterios para la estratigrafía del Neopaleozoico de la sierra de Los Llanos, La Rioja, República Argentina: Boletín de la Academia Nacional de Ciencias, v. 57, no. 11–2, p. 1–119. Córdoba.
- Azcuy, C., 1975, Miosporas del Namuriano y Westfaliano de la comarca Malanzán-Loma Larga, provincia de La Rioja, Argentina: I. Localización geográfica y geológica de la comarca y descripciones sistemáticas: Ameghiniana, v. 12, no. 1, p. 1–69.
- Azcuy, C., and Morelli, J., 1970, Geología de la comarca Paganzo-Amana. El Grupo Paganzo. Formaciones que lo componen y sus relaciones: Revista de la Asociación Geológica Argentina v. XXV, p. 405–429.
- Báez, M.A., Basei, M.A.S., Rossi, J., and Toselli, A.J., 2008, Geochronology of Paleozoic magmatic events in northern Sierra de Velasco, Argentina, in Linares, E., et al, eds, 6th South American Symposium on Isotopic Geology: San Carlos de Bariloche, Argentina, INGEIS, Buenos Aires, p. 66.
- Baldo, E.G., Demange, M., and Martino, R.D., 1996, Evolution of the Sierras de Córdoba, Argentina: Tectonophysics, v. 267, p. 121–142, doi:10.1016/S0040-1951(96)00092-3.
- Barazangi, M., and Isacks, B., 1976, Spatial distribution of earthquakes and subduction of the Nazca plate beneath South America: Geology, v. 4, p. 686–692, doi:10.1130/0091-7613(1976)4<686:SDOEAS>2.0.CO;2.
- Barazangi, M., and Isacks, B., 1979, Subduction of the Nazca plate beneath Peru: Evidence from spatial distribution of earthquakes: Geophysical Journal of the Royal Astronomical Society, v. 57, p. 537–555, doi:10.1111/j.1365-246X.1979.tb06778.x.
- Bernet, M., and Garver, J.I., 2005, Fission-track analysis of Detrital zircon, in Reiners, P.W., and Ehlers, T.A., eds., Low-Temperature Thermochronology: Techniques, Interpretations, and Applications: Reviews in Mineralogy and Geochemistry, v. 58, p. 205–237.
- Bernet, M., Brandon, M.T., Garver, J.I., and Molitor, B., 2004, Downstream changes of alpine zircon fission-track ages in the Rhone and Rhine Rivers: Journal of Sedimentary Research, v. 74, p. 82–94, doi:10.1306/041003740082.
- Bernet, M., van der Beek, P., Pik, R., Huyghez, P., Mugnier, J.L., Labrinz, E., and Szulc, A., 2006, Miocene to Recent exhumation of the central Himalaya determined from combined detrital zircon fission-track and U-Pb analysis of Siwalik sediments, western Nepal: Basin Research, v. 18, p. 393–412, doi:10.1111/j.1365-2117.2006.00303.x.
- Bernet, M., Brandon, M., Garver, J., Balestrieri, M.L., Ventura, B., and Zattin, M., 2009, Exhuming the Alps through time: Clues from detrital zircon fission-track thermochronology: Basin Research, v. 21, p. 781–798, doi:10.1111/j.1365-2117.2009.00400.x.
- Blythe, A.E., Burbank, D.W., Carter, A., Schmidt, K., and Putkonen, J., 2007, Plio-Quaternary exhumation history of the central Nepalese Himalaya: 1. Apatite and zircon fission track and apatite [U-Th]/He analyses: Tectonics, v. 26, p. TC3002, doi:10.1029/2006TC001990.
- Bracaccini, O., 1946, Los estratos de Paganzo y sus niveles plantíferos en la sierra de Los Llanos (provincia de La Rioja): Revista de la Sociedad Geológica Argentina, v. 1, no. 1, p. 19–61.
- Brandon, M.T., 1992, Decomposition of fission-track grain-age distributions: American Journal of Science, v. 292, p. 535–564, doi:10.2475/ajs.292.8.535.
- Brandon, M.T., 1996, Probability density plot for fission track grain-age samples: Radiation Measurements, v. 26, p. 663–676, doi:10.1016/S1350-4487(97)82880-6.
- Brandon, M.T., Roden-Tice, M.K., and Garver, J.I., 1998, Late Cenozoic exhumation of the Cascadia accretionary wedge in the Olympic Mountains, northwest Washington State: Geological Society of America Bulletin, v. 110, p. 985–1009, doi:10.1130/0016-7606(1998)110<0985:LCETOC>2.3.CO;2.
- Carignano, C., Cioccale, M., and Rabassa, J., 1999, Landscape antiquity of the central-eastern Sierras Pampeanas (Argentina): Geomorphological evolution since Gondwanic times: Zeitschrift für Geomorphologie Neue Folge, v. 118, p. 245–268.
- Carlson, W.D., Donelick, R.A., and Ketcham, R.A., 1999, Variability of apatite fission track annealing kinetics: I. Experimental results: The American Mineralogist, v. 84, p. 1213–1223.
- Carter, A., 1990, The thermal history and annealing effects of zircons from the Ordovician of North Wales: Nuclear Tracks and Radiation Measurements, v. 17, p. 309–313, doi:10.1016/1359-0189(90)90051-X.
- Collo, G., Dávila, F.M., Nóbile, J., Astini, R.A., and Gehrels, G., 2011, Clay mineralogy and thermal history of the Neogene Vinchina Basin, central Andes of Argentina: Analysis of factors controlling the heating conditions: Tectonics, v. 30, p. TC4012, doi:10.1029/2010TC002841.
- Coughlin, T.J., O'Sullivan, P.B., Kohn, B.P., and Holcombe, R.J., 1998, Apatite fission-track thermochronology of the Sierras Pampeanas, central western Argentina: Implications for the mechanism of plateau uplift in the Andes: Geology, v. 26, p. 999–1002, doi:10.1130/0091-7613(1998)026<0999:AFTTOT>2.3.CO;2.
- Crisafulli, A., and Herbst, R., 2008, Maderas gimnospermas de la Formación Solca (Pérmico Inferior), provincia de La Rioja, Argentina: Ameghiniana, v. 45, no. 4, p. 737–751.
- Cuerda, A.J., 1965, Estratigrafía de los depósitos Neopaleozoicos de la sierra de Maz (provincia de La Rioja), 2º: Jornadas Geológicas Argentinas (Salta 1963): Actas, v. 3, p. 79–94.
- Dahlquist, J.A., Rapela, C.W., and Baldo, E.G., 2005, Petrogenesis of cordierite-bearing S-type granitoids in Sierra de Chepes, Famatinian orogen, Argentina: Journal of South American Earth Sciences, v. 20, p. 231–251, doi:10.1016/j.jsames.2005.05.014.
- Dahlquist, J.A., Galindo, C., Pankhurst, R.J., Rapela, C.W., Alasino, P.H., Saavedra, J., and Fanning, C.M., 2007, Magmatic evolution of the Peñón Rosado granite: Petrogenesis of garnet-bearing granitoids: Lithos, v. 95, p. 177–207, doi:10.1016/j.lithos.2006.07.010.
- Dahlquist, J.A., Pankhurst, R.J., Rapela, C.W., Galindo, C., Alasino, P., Fanning, C.M., Saavedra, J., and Baldo, E., 2008, New SHRIMP U-Pb data from the Famatina complex: Constraining Early–Mid-Ordovician Famatinian magmatism in the Sierras Pampeanas, Argentina: Geologica Acta, v. 6, p. 319–333.
- Davila, F.M., and Carter, A., 2013, Exhumation history of the Andean broken foreland revisited: Geology, v. 41, p. 443–446, doi:10.1130/G33960.1.
- de los Hoyos, C.R., Willner, A.P., Larrovere, M.A., Rossi, J.N., Toselli, A.J., and Basei, M.A.S., 2011, Tectonothermal evolution and exhumation history of the Paleozoic proto-Andean Gondwana margin crust: The Famatinian belt in NW Argentina: Gondwana Research, v. 20, p. 309–324, doi:10.1016/j.gr.2010.12.004.
- Dodson, M.H., 1973, Closure temperature in cooling geochronological and petrological systems: Contributions to Mineralogy and Petrology, v. 40, p. 259–274, doi:10.1007/BF00373790.
- Donelick, R.A., and O'Sullivan, P.B., 2005, Apatite fission track analysis: Reviews in Mineralogy and Geochemistry, v. 58, p. 49–94, doi:10.2138/rmg.2005.58.3.
- Drobe, M., López de Luchi, M., Steenken, A., Frei, R., Naumann, R., Siegesmund, S., and Wemmer, K., 2009, Provenance of the Late Proterozoic to Early Cambrian metaclastic sediments of the Sierra de San Luis (eastern Sierras Pampeanas) and Cordillera Oriental, Argentina: Journal of South American Earth Sciences, v. 28, p. 239–262, doi:10.1016/j.jsames.2009.06.005.
- Drobe, M., de Luchi, M.L., Steenken, A., Wemmer, K., Naumann, R., Frei, R., and Siegesmund, S., 2011, Geodynamic evolution of the Eastern Sierras Pampeanas (central Argentina) based on geochemical, Sm-Nd, Pb-Pb and SHRIMP data: International Journal of Earth Sciences, v. 100, no.2, p. 631–657, doi:10.1007/s00531-010-0593-3.
- Enkelmann, E., Zettler, P.K., Garver, J.I., Pavlis, T.L., and Hooks, B.P., 2010, The thermochronological record of tectonic and surface process interaction at the Yakutat–North American collision zone in southeast Alaska: American Journal of Science, v. 310, p. 231–260, doi:10.2475/04.2010.01.
- Enkelmann, E., Ehlers, T.A., Zettler, P.K., and Hallet, B., 2011, Denudation of the Namche Barwa antiform, Eastern Himalaya: Earth and Planetary Science Letters, v. 307, p. 323–333, doi:10.1016/j.epsl.2011.05.004.
- Farley, K.A., 2002, (U-Th)/He dating: Techniques, calibration, and applications, in Porcelli, D., Ballentine, C.J., and Wieler, R., eds, Noble Gases in Geochemistry and Cosmochemistry: Reviews in Mineralogy and Geochemistry, v. 47, p. 819–844.
- Fernandez-Seveso, F., and Tankard, A.J., 1995, Tectonics and stratigraphy of the late Paleozoic Paganzo basin of western Argentina and its regional implications, in Tankard, A., Suarez Soruco, R., and Welsink, H.J., eds., Petroleum Basins of South America: American Association of Petroleum Geologists Memoir 62, p. 285–304.
- Fiorelli, L.E., Grellet-Tinner, G., Argañaraz, E., Larrovere, M.A., Chornogubsky, L., Torrens, J., and Hechenleitner, E.M., 2011, Record of the first Cretaceous continental fauna from La Rioja Province, northwestern Argentina: Geopaleontological Implications, in 22nd Latinamerika-Kolloquium 2011, Heidelberg, Germany, Abstracts and Program (2011), p. 83.
- Fisher, N.D., Jordan, T.E., and Brown, L., 2002, The structural and stratigraphic evolution of the La Rioja basin, Argentina: Journal of South American Earth Sciences, v. 15, p. 141–156, doi:10.1016/S0895-9811(02)00010-X.
- Fitzgerald, P.G., Baldwin, S.L., Webb, L.E., and O'Sullivan, P.B., 2006, Interpretation of (U-Th)/He single grain ages from slowly cooled crustal terranes: A case study from the Transantarctic Mountains of southern Victoria

- Land: *Chemical Geology*, v. 225, p. 91–120, doi:10.1016/j.chemgeo.2005.09.001.
- Flowers, R.M., Wernicke, B.P., and Farley, K.A., 2008, Unroofing, incision, and uplift history of the southwestern Colorado Plateau from apatite (U-Th)/He thermochronometry: *Geological Society of America Bulletin*, v. 120, p. 571–587, doi:10.1130/B26231.1.
- Frei, D., and Gerdes, A., 2009, Precise and accurate in situ U-Pb dating of zircon with high sample throughput by automated LA-SF-ICP-MS: *Chemical Geology*, v. 261, p. 261–270, doi:10.1016/j.chemgeo.2008.07.025.
- Freguelli, J., 1944, Apuntes acerca del Paleozoico Superior del noroeste Argentino: *Revista del Museo de La Plata, Nueva Serie: Geología*, v. 2, no. 15, p. 213–265.
- Galbraith, R.F., and Green, P.F., 1990, Estimating the component ages in a finite mixture: *Nuclear Tracks and Radiation Measurements*, v. 17, p. 197–206, doi:10.1016/1359-0189(90)90035-V.
- Galbraith, R.F., and Laslett, G.M., 1993, Statistical models for mixed fission track ages: *Nuclear Tracks and Radiation Measurements*, v. 21, p. 459–470, doi:10.1016/1359-0189(93)90185-C.
- Garver, J.I., Brandon, M.T., Roden-Tice, M.K., and Kamp, P.J.J., 1999, Exhumation history of orogenic highlands determined by detrital fission track thermochronology, in Ring, U., Brandon, M.T., Lister, G.S., and Willett, S.D., eds., *Exhumation Processes: Normal Faulting, Ductile Flow, and Erosion*: Geological Society of London Special Publication 54, p. 283–304.
- Garver, J.I., Riley, B.C.D., and Wang, G., 2002, Partial resetting of fission tracks in detrital zircon (European Fission-Track Conference, Cadiz, Spain): *Geotemas*, v. 4, p. 73–75.
- Garver, J.I., Reiners, P.W., Walker, L.J., Ramage, J.M., and Perry, S.E., 2005, Implications for timing of Andean uplift from thermal resetting of radiation damaged zircon in the Cordillera Huayhuash, northern Peru: *The Journal of Geology*, v. 113, p. 117–138, doi:10.1086/427664.
- Gleadow, A.J.W., Duddy, I.R., Green, P.F., and Lovering, J.F., 1986, Confined fission track length in apatite: A diagnostic tool for thermal history analysis: *Contributions to Mineralogy and Petrology*, v. 94, p. 405–415, doi:10.1007/BF00376334.
- González, P.D., Sato, A.M., Llambías, E.J., Basei, M.A.S., and Vlach, S.R.F., 2004, Early Paleozoic structural and metamorphic evolution of western Sierra de San Luis (Argentina), in relation to Cuyania accretion: *Gondwana Research*, v. 7, p. 1157–1170, doi:10.1016/S1342-937X(05)71091-1.
- González, R.R., and Toselli, A.J., 1975, La efusividad del Mesozoico argentino y su relación con áreas sudamericanas. *Annals XXV Congreso Brasileiro de Geologia: São Paulo, Brasil*, p. 259–272.
- Green, P.F., Duddy, I.R., Gleadow, A.J.W., Tingate, P.T., and Laslett, G.M., 1986, Thermal annealing of fission tracks in apatite: 1. A qualitative description: *Isotope Geoscience*, v. 59, p. 237–253, doi:10.1016/0168-9622(86)90074-6.
- Green, P.F., Duddy, I.R., Laslett, G.M., Hegarty, K.A., Gleadow, A.J.W., and Lovering, J.F., 1989, Thermal annealing of fission tracks in apatite: 4. Quantitative modeling techniques and extension to geological timescales: *Chemical Geology*, v. 79, p. 155–182.
- Gulbranson, E.L., Montañez, I.P., Schmitz, M.D., Limarino, C.O., Isbell, J.L., Marenssi, S.A., and Crowley, J.L., 2010, High-precision U-Pb calibration of Carboniferous glaciation and climate history, Paganzo Group, NW Argentina: *Geological Society of America Bulletin*, v. 122, no. 9/10, p. 1480–1498, doi:10.1130/B30025.1.
- Hacker, B.R., Kelemen, P.B., Rioux, M., McWilliams, M.O., Gans, P.B., Reiners, P.W., Layer, P.W., Söderlund, U., and Vervoort, J.D., 2011, Thermochronology of the Talkeetna intraoceanic arc of Alaska: *Ar/Ar, U-Th/He, Sm-Nd, and Lu-Hf* dating: *Tectonics*, v. 30, p. TC1011, doi:10.1029/2010TC002798.
- Hendriks, B., Andriessen, P., Huigen, Y., Leighton, C., Redfield, T., Murrell, G., Gallagher, K., and Nielsen, S.B., 2007, A fission track data compilation for Fennoscandia: *Norwegian Journal of Geology*, v. 87, p. 143–155. ISSN 029–196X.
- Höckenreiner, M., Söllner, F., and Miller, H., 2003, Dating the TIPA shear zone: An Early Devonian terrane boundary between the Famatinian and Pampean system (NW Argentina): *Journal of South American Earth Sciences*, v. 16, p. 45–66, doi:10.1016/S0895-9811(03)00018-X.
- House, M.A., Gurnis, M., Sutherland, R., and Kamp, P.J.J., 2005, Patterns of late Cenozoic exhumation deduced from apatite and zircon U-He ages from Fiordland, New Zealand: *Geochemistry Geophysics Geosystems*, v. 6, p. Q09013, doi:10.1029/2005GC000968.
- Jonckheere, R., Ratschbacher, L., and Wagner, G.A., 2003, A repositioning technique for counting induced fission tracks in muscovite external detectors in single-grain dating of minerals with low and inhomogeneous uranium concentrations: *Radiation Measurements*, v. 37, p. 217–219, doi:10.1016/S1350-4487(03)00029-5.
- Jordan, T.E., Zeitler, P., Ramos, V., and Gleadow, A.J.W., 1989, Thermochronometric data on the development of the basement peneplain in the Sierras Pampeanas, Argentina: *Journal of South American Earth Sciences*, v. 2, p. 207–222, doi:10.1016/0895-9811(89)90030-8.
- Kleiman, L.E., and Japas, M.S., 2009, The Choyoi volcanic province at 34°–36°S (San Rafael, Mendoza, Argentina): Implications for the late Paleozoic evolution of the southwestern margin of Gondwana: *Tectonophysics*, v. 473, p. 283–299, doi:10.1016/j.tecto.2009.02.046.
- Limarino, C., Tripaldi, A., Marenssi, S., and Fauqué, L., 2006, Tectonic, sea-level, and climatic controls on late Paleozoic sedimentation in the western basins of Argentina: *Journal of South American Earth Sciences*, v. 22, p. 205–226, doi:10.1016/j.jsames.2006.09.009.
- Lisker, F., Läufer, A.L., Olesch, M., Rossetti, F., and Schäfer, T., 2006, Transantarctic Basin: New insights from fission track and structural data from the USARP Mountains and adjacent areas (Northern Victoria Land, Antarctica): *Basin Research*, v. 18, p. 497–520, doi:10.1111/j.1365-2117.2006.00301.x.
- Löbels, S., Bense, F.A., Wemmer, K., Dunkl, I., Costa, C.H., Layer, P., and Siegesmund, S., 2011, Exhumation and uplift of the Sierras Pampeanas: Preliminary implications from K-Ar fault gouge dating and low-T thermochronology in the Sierra de Comechingones (Argentina): *International Journal of Earth Sciences*, v. 100, p. 671–694, doi:10.1007/s00531-010-0608-0.
- López de Luchi, M.G., Siegesmund, S., Wemmer, K., Steenken, A., and Naumann, R., 2007, Geochemical constraints on the petrogenesis of the Paleozoic granitoids of the Sierra de San Luis, Sierras Pampeanas, Argentina: *Journal of South American Earth Sciences*, v. 24, p. 138–166, doi:10.1016/j.jsames.2007.05.001.
- López-Gamundi, O.R., 2006, Permian plate margin volcanism and tuffs in adjacent basins of west Gondwana: Age constraints and common characteristics: *Journal of South American Earth Sciences*, v. 22, p. 227–238, doi:10.1016/j.jsames.2006.09.012.
- Ludwig, K.R., 2001, *Users Manual for Isoplot/Ex Rev. 2.49*: Berkeley Geochronology Center Special Publication 1a, 56 p.
- Martino, R.D., 1999, La faja de deformación Sauce Punco, sierra Norte, Córdoba, Argentina: *Revista de la Asociación Geológica Argentina*, v. 53, p. 436–440.
- McDougall, I., and Harrison, T.M., 1999, *Geochronology and Thermochronology by the ⁴⁰Ar/³⁹Ar Method*: Oxford, UK, Oxford University Press, 267 p.
- Milana, J.P., and Alcober, O., 1994, Tectosedimentary model of the Triassic Ischigualasto Basin, San Juan: Argentina: *Revista de la Asociación Geológica Argentina*, v. 49, no. 3–4, p. 217–235.
- Mpodozis, C., and Kay, S.M., 1992, Late Paleozoic to Triassic evolution of the Gondwana margin: Evidence from Chilean Frontal Cordilleran batholiths (28° to 31°S): *Geological Society of America Bulletin*, v. 104, p. 999–1014, doi:10.1130/0016-7606(1992)104<0999:LPTTEO>2.3.CO;2.
- Net, L.I., and Limarino, C.O., 1999, Paleogeografía y correlación estratigráfica del Paleozoico Superior de la Sierra de Los Llanos, provincia de La Rioja, Argentina: *Revista de la Asociación Geológica Argentina*, v. 54, p. 229–239.
- Net, L.I., and Limarino, C.O., 2006, Applying sandstone petrofacies to unravel the Upper Carboniferous evolution of the Paganzo Basin, northwest Argentina: *Journal of South American Earth Sciences*, v. 22, p. 239–254, doi:10.1016/j.jsames.2006.09.010.
- Omarini, R.H., 1983, Caracterización Litológica, Diferenciación y Génesis de la Formación Puncovicosa entre el Valle de Lerma y la Faja Eruptiva de la Puna [Ph.D. thesis]: Salta, Argentina, Universidad Nacional de Salta, 202 p.
- Pankhurst, R.J., Rapela, C.W., Saavedra, J., Baldo, E., Dahlquist, J., Pascua, I., and Fanning, C.M., 1998, The Famatinian magmatic arc in the Central Sierras Pampeanas: An early to mid-Ordovician continental arc on the Gondwana margin, in Pankhurst, R.J., and Rapela, C.W., eds., *The Proto-Andean Margin of Gondwana*: Geological Society of London Special Publication 142, p. 343–367.
- Rahn, M.K., Brandon, M.T., Batt, G.E., and Garver, J.I., 2004, A zero-damage model for fission-track annealing in zircon: *The American Mineralogist*, v. 89, p. 473–484.
- Ramos, V.A., 2010, The tectonic regime along the Andes: Present-day and Mesozoic regimes: *Geological Journal*, v. 45, p. 2–25, doi:10.1002/gj.1193.
- Ramos, V.A., Jordan, T.E., Allmendinger, W., Mpodozis, C., Kay, S.M., Cortés, J.M., and Palma, M., 1986, Paleozoic terranes of the central Argentine-Chilean Andes: *Tectonics*, v. 5, p. 855–880, doi:10.1029/TC005i06p00855.
- Ramos, V.A., Cristallini, E.O., and Perez, D.J., 2002, The Pampean flat-slab of the Central Andes: *Journal of South American Earth Sciences*, v. 15, p. 59–78, doi:10.1016/S0895-9811(02)00066-8.
- Ramos, V.A., Vujovich, G., Martino, R., and Otamendi, J., 2010, Pampia: A large cratonic block missing in the Rodinia supercontinent: *Journal of Geodynamics*, v. 50, p. 243–255, doi:10.1016/j.jog.2010.01.019.
- Rapela, C.W., Pankhurst, R.J., Casquet, C., Baldo, E., Saavedra, J., Galindo, C., and Fanning, C.M., 1998, The Pampean orogeny of the southern proto-Andes: Evidence for Cambrian continental collision in the Sierras de Córdoba, in Pankhurst, R.J., and Rapela, C.W., eds., *The Proto-Andean Margin of Gondwana*: Geological Society of London Special Publication 142, p. 181–217.
- Rapela, C.W., Pankhurst, R., Baldo, E., Casquet, C., Galindo, C., Fanning, C., and Saavedra, J., 2001, Ordovician metamorphism in the Sierras Pampeanas: New U-Pb SHRIMP ages in central-east Valle Fértil and the Velasco batholith, in 3rd South American Symposium on Isotope Geology, p. 616–619.
- Rapela, C.W., Pankhurst, R.J., Casquet, C., Fanning, C.M., Baldo, E.G., Gonzalez-Casado, J.M., Galindo, C., and Dahlquist, J., 2007, The Rio de la Plata craton and the assembly of SW Gondwana, *Earth Science Review*, 83, p. 49–82.
- Reiners, P.W., Farley, K.A., and Hicke, H.J., 2002, He diffusion and (U-Th)/He thermochronometry of zircon: Initial results from Fish Canyon Tuff and Gold Butte: *Tectonophysics*, v. 349, p. 297–308, doi:10.1016/S0040-1951(02)00058-6.
- Reiners, P.W., Spell, T.L., Nicolescu, S., and Zanetti, K.A., 2004, Zircon (U-Th)/He thermochronometry: He diffusion and comparison with ⁴⁰Ar/³⁹Ar dating: *Geochimica et Cosmochimica Acta*, v. 68, p. 1857–1887, doi:10.1016/j.gca.2003.10.021.
- Richardson, T., Gilbert, H., Anderson, M., and Ridgway, K.D., 2012, Seismicity within the actively deforming Eastern Sierras Pampeanas, Argentina: *Geophysical Journal International*, v. 188, p. 408–420, doi:10.1111/j.1365-246X.2011.05283.x.
- Richardson, T., Ridgway, K.D., Gilbert, H., Martino, R., Enkelmann, E., Anderson, M., and Alvarado, P., 2013, Neogene and Quaternary tectonics of the Eastern Sierras Pampeanas, Argentina: Active intraplate deformation inboard of flat-slab subduction: *Tectonics*, v. 32, p. 780–796, doi:10.1002/tect.20054.
- Rocha-Campos A.C., Basei, M.A., Nutman, A.P., Kleiman, L.E., Varela, R., Llambías, E., Canile, F.M., and da Rosa, O., de C.R., 2011, 30 million years of Permian volcanism recorded in the Choyoi igneous province (W Argentina) and their source for younger ash fall deposits in the Paraná Basin: SHRIMP U-Pb zircon geochronology evidence: *Gondwana Research*, v. 19, p. 509–523.
- Roden-Tice, M.K., and Tice, S.J., 2005, Regional-scale mid-Jurassic to Late Cretaceous unroofing from the Adirondack Mountains through central New England based on apatite fission-track and (U-Th)/He thermochronology: *The Journal of Geology*, v. 113, p. 535–552, doi:10.1086/431908.
- Schwartz, J.J., and Gromet, L.P., 2004, Provenance of the Late Proterozoic–Early Cambrian basin, Sierras de Cor-

- doba, Argentina: *Precambrian Research*, v. 129, p. 1–21, doi:10.1016/j.precamres.2003.08.011.
- Schwartz, J.J., Gromet, L.P., and Miró, R., 2008, Timing and duration of the calc-alkaline arc of the Pampean orogeny: Implication for the Late-Neoproterozoic to Cambrian evolution of western Gondwana: *The Journal of Geology*, v. 116, p. 39–61, doi:10.1086/524122.
- Seward, D., and Rhodes, D.A., 1986, A clustering technique for fission track dating of fully to partially annealed mineral and other non-unique populations: *Nuclear Tracks and Radiation Measurements*, v. 11, p. 259–268, doi:10.1016/1359-0189(86)90043-9.
- Shuster, D.L., Ehlers, T.A., Rusmore, M.E., and Farley, K.A., 2005, Rapid glacial erosion at 1.8 Ma revealed by ⁴He/³He thermochronometry: *Science*, v. 310, p. 1668–1670, doi:10.1126/science.1118519.
- Shuster, D.L., Flowers, R.M., and Farley, K.A., 2006, The influence of natural radiation damage on helium diffusion kinetics in apatite: *Earth and Planetary Science Letters*, v. 249, p. 148–161, doi:10.1016/j.epsl.2006.07.028.
- Siegesmund, S., Steenken, A., López de Luchi, M.G., Wemmer, K., Hoffmann, A., and Mosch, S., 2004, The Las Chacras-Potrillo batholith (Pampean Range, Argentina): Structural evidence, emplacement and timing of the intrusion: *International Journal of Earth Sciences*, v. 93, p. 23–43, doi:10.1007/s00531-003-0363-6.
- Siegesmund, S., Steenken, A., Martino, R.D., Wemmer, K., López de Luchi, M.G., Frei, R., Presnyakov, S., and Guerschi, A., 2010, Time constraints on the tectonic evolution of the Eastern Sierras Pampeanas (Central Argentina): *International Journal of Earth Sciences*, v. 99, p. 1199–1226, doi:10.1007/s00531-009-0471-z.
- Sims, J.P., Ireland, T.R., Camacho, A., Lyons, P., Pieters, P.E., Skirrow, R.G., Stuart-Smith, P.G., and Miró, R., 1998, U-Pb, Th-Pb and Ar-Ar geochronology from the southern Sierras Pampeanas, Argentina: Implications for the Palaeozoic tectonic evolution of the western Gondwana margin, in Pankhurst, R.J., and Rapela, C.W., eds., *The Proto-Andean Margin of Gondwana*: Geological Society of London Special Publication 142, p. 259–281.
- Socha, B.J., Carignano, C., Rabassa, J., and Mickelson, D.M., 2006, Sedimentological record of Carboniferous mountain glaciation in an exhumed paleovalley, eastern Paganzo Basin, La Rioja Province: *Geological Society of America Abstracts with Programs*, v. 38, no. 7, p. 62.
- Söllner, F., Brodtkorb, M., Miller, H., Pezutti, N., and Fernández, R., 2000, U-Pb zircon ages of metavolcanic rocks from the Sierra de San Luis, Argentina: *Revista de la Asociación Geológica Argentina*, v. 55, p. 15–22.
- Spotila, J.A., and Berger, A.L., 2010, Exhumation at orogenic indenter corners under long-term glacial conditions: Example of the St. Elias orogen, southern Alaska: *Tectonophysics*, v. 490, p. 241–256, doi:10.1016/j.tecto.2010.05.015.
- Stacey, J.S., and Kramers, J.D., 1975, Approximation of terrestrial lead isotope evolution by a two-stage model: *Earth and Planetary Science Letters*, v. 26, p. 207–221, doi:10.1016/0012-821X(75)90088-6.
- Steenken, A., López de Luchi, M.G., Siegesmund, S., Wemmer, K., and Pawlig, S., 2004, Crustal provenance and cooling of the basement complexes of the Sierra de San Luis: An insight into the tectonic history of the proto-Andean margin of Gondwana: *Gondwana Research*, v. 7, no. 4, p. 1171–1195, doi:10.1016/S1342-937X(05)71092-3.
- Steenken, A., Siegesmund, S., López de Luchi, M.G., Frei, R., and Wemmer, K., 2006, Neoproterozoic to early Palaeozoic events in the Sierra de San Luis: Implications for the Famatinian geodynamics in the Eastern Sierras Pampeanas (Argentina): *Journal of the Geological Society of London*, v. 163, p. 965–982, doi:10.1144/0016-76492005-064.
- Steenken, A., Siegesmund, S., Wemmer, K., and López de Luchi, M.G., 2008, Time constraints on the Famatinian and Achalian structural evolution of the basement of the Sierra de San Luis (Eastern Sierras Pampeanas, Argentina): *Journal of South American Earth Sciences*, v. 25, p. 336–358, doi:10.1016/j.jsames.2007.05.002.
- Steenken, A., Wemmer, K., Martino, R.D., López de Luchi, M.G., Guerschi, A., and Siegesmund, S., 2010, Post-Pampean cooling and the uplift of the Sierras Pampeanas in the west of Córdoba (Central Argentina): *Neue Jahrbuch Geologische Paläontologische Abhandlungen*, v. 256, p. 235–255, doi:10.1127/0077-7749/2010/0094.
- Sterren, A., and Martínez, M., 1996, El paleovalle de Olta (Carbonífero) Paleoaambiente y paleogeografía, in XIII Argentine Geological Congress: *Asociación Geológica Argentina (AGA)*, Buenos Aires, Argentina, *Actas*, v. 11, p. 89–103.
- Stipanovic, P.N., 2002, El Triásico en la Argentina, in Stipanovic, P.N., and Marsicano, C.A., eds., *Léxico Estratigráfico de la Argentina*, Volume 3, Triásico: *Asociación Geológica Argentina*, ser. B (Didáctica y Complementaria), v. 26, p. 1–24.
- Stock, G.M., Ehlers, T.A., and Farley, K.A., 2006, Where does sediment come from? Quantifying catchment erosion with detrital apatite (U-Th)/He thermochronometry: *Geology*, v. 34, no. 9, p. 725–728, doi:10.1130/G22592.1.
- Strazzere, L., Gregori, D., and Dristas, J.A., 2006, Genetic evolution of Permian–Triassic volcanoclastic sequences at Uspallata, Mendoza Precordillera, Argentina: *Gondwana Research*, v. 9, p. 485–499, doi:10.1016/j.gr.2005.12.003.
- Stuart-Smith, P.G., Miró, R., Sims, J.P., Pieters, P.E., Lyons, P., Camacho, A., Ireland, T.R., Skirrow, R.G., and Black, L.P., 1999, Uranium-lead dating of felsic magmatic cycles in the southern Sierras Pampeanas, Argentina: Implications for the tectonic development of the proto-Andean Gondwana margin, in Ramos, V.A., and Kerppe, J.D., eds., *Laurentia-Gondwana Connection before Pangea*: Geological Society America Special Paper 336, p. 87–114.
- Tagami, T., Galbraith, R.F., Yamada, R., and Laslett, G.M., 1998, Revised annealing kinetics of fission tracks in zircon and geological implications, in Van den haute, P., and De Corte, F., eds., *Advances in Fission-Track Geochronology*: Dordrecht, Netherlands, Kluwer Academic Publisher, p. 99–112.
- Thiede, R.C., Ehlers, T.A., Bookhagen, B., and Strecker, M.R., 2009, Erosional variability along the northwest Himalaya: *Journal of Geophysical Research*, v. 114, p. F01015, doi:10.1029/2008JF001010.
- Toselli, A.J., and Aceñolaza, F.G., 1978, Geocronología de las Formaciones Puncovicana y Suncho, Provincias de Salta y Catamarca: *Revista de la Asociación Geológica Argentina*, v. 33, p. 76–80.
- Uliana, M.A., and Biddle, K.T., 1988, Mesozoic–Cenozoic paleogeographic, geodynamic evolution of southern South America: *Revista Brasileira de Geociencias*, v. 18, p. 172–190.
- Uliana, M.A., Biddle, K.T., and Cerdán, J., 1989, Mesozoic extension and the formation of Argentine sedimentary basin, in Tankard, A.J., and Balkwill, H.R., eds., *Extensional Tectonics and Stratigraphy of the North Atlantic Margins*: American Association of Petroleum Geologists Memoir 46, p. 509–614.
- Valencio, D.A., Mendía, J.E., and Vilas, J.F., 1975, Palaeomagnetism and K-Ar ages of Triassic igneous rocks from the Ischigualasto-Ischichuca Basin and Puesto Viejo Formation, Argentina: *Earth and Planetary Science Letters*, v. 26, no. 3, p. 319–330, doi:10.1016/0012-821X(75)90007-2.
- Willett, S.D., Fisher, D., Fuller, C., En-Chao, Y., and Chia-Yu, L., 2003, Erosion rates and orogenic-wedge kinematics in Taiwan inferred from fission-track thermochronometry: *Geology*, v. 31, no. 11, p. 945–948, doi:10.1130/G19702.1.
- Yamada, R., Tagami, T., Nishimura, S., and Ito, H., 1995, Annealing kinetics of fission tracks in zircon: An experimental study: *Chemical Geology*, v. 122, p. 249–258, doi:10.1016/0009-2541(95)00006-8.
- Zeitler, P.K., Koons, P.O., Bishop, M.L., Chamberlain, C.P., Craw, D., Edwards, M.A., Hamidullah, S., Jan, M.Q., Khan, M.A., Khattak, M.U.K., Kidd, W.S.F., Mackie, R.L., Meltzer, A.S., Park, S.K., Pecher, A., Poage, M.A., Sarker, G., Schneider, D.A., Seeber, L., and Shroder, J., 2001, Crustal reworking at Nanga Parbat, Pakistan: Metamorphic consequences of thermal-mechanical coupling facilitated by erosion: *Tectonics*, v. 20, p. 712–728, doi:10.1029/2000TC001243.
- Zerfass, H., Chemale, F., Jr., Schultz, C.L., and Lavina, E., 2004, Tectonics and sedimentation in southern South America during Triassic: *Sedimentary Geology*, v. 166, p. 265–292, doi:10.1016/j.sedgeo.2003.12.008.

MANUSCRIPT RECEIVED 15 JULY 2013
 REVISED MANUSCRIPT RECEIVED 27 JANUARY 2014
 MANUSCRIPT ACCEPTED 07 FEBRUARY 2014

Printed in the USA